





Analysis of Mathematical Listeriosis Model in Ready-to-Eat Food

Kapil Toor^{1,†, }, Kalyan Das^{2,‡,*, }, M N Srinivas^{3,||, } and Anushaya Mohapatra^{4,§, }



^{1,2}Department of Interdisciplinary Sciences, National Institute of Food Technology Entrepreneurship and Management, Kundli, Haryana, India

³Department of Mathematics, School of Advanced Sciences, Vellore Institute of Technology, Vellore, Tamilnadu, India

⁴Department of mathematics, BITS Pilani, K.K Birla Goa Campus, Goa, India

[†]kake@iit.tsukuba.ac.jp, [‡]daskalyan27@gmail.com, ^{||}mnsrinivaselr@gmail.com,

[§]anushayam@goa.bits-pilani.ac.in,

*Corresponding author

Doi: <https://doi.org/10.33401/jome.1630459>

Abstract: This study emphasis on transmission of Listeriosis from ready-to-eat foods employing a four compartment defined as classes like susceptible $S(t)$, Exposed $E(t)$, Infected $I(t)$ and Recovered $R(t)$ of non-linear model. Some RTE foods contains Listeria Which causes Listeriosis. we proposed four compartmental model and analysis of equilibrium point, one is disease free equilibrium point (DFE) and Endemic equilibrium points. Local stability of equilibrium established. The findings of this research work could be used to provide basis in order to curb Listeriosis from ready-to-eat processed food items. This study analyzes a mathematical model designed to understand the dynamics of listeriosis transmission through ready-to-eat (RTE) foods. The model integrates factors such as cross-contamination in food processing environments and the role of contaminated food products in spreading the disease. It categorizes the system into three equilibria: disease-free, Listeria-free, and endemic states. The analysis reveals that controlling listeriosis effectively requires the removal of contaminated food products and reducing environmental contamination. The model's findings support the development of optimal control strategies to mitigate listeriosis outbreaks associated with RTE foods

Keywords: RTE Model; Mathematical model; Basic reproduction number; Contaminated food products; Listeria monocytogene. **AMS Math Codes:** xxxx; xxxxx; xxxxx.

1. Introduction

Listeria monocytogenes, is often linked to the intake of ready-to-eat food with contamination which is major cause of Listeriosis. The study of infectious disease dynamics has been a crucial area of research in epidemiology, aiming to learn and control, the development of diseases within populations. This report is inspired by the work presented in the paper titled *A Mathematical Model and Optimal Control for Listeriosis Disease from Ready-to-Eat Food Products*. The paper formulates a mathematical model using the classic SIR (Susceptible-Infectious-Recovered) framework to describe The causes and effects of listeriosis progression in the context of food products which are ready-to-eat. In the pursuit of extending and enhancing the existing model, this project introduces an Exposed (E) compartment, transforming the SIR model into an SEIR (Susceptible-Exposed-Infectious-Recovered) model. The addition of an Exposed compartment allows for the incorporation of an incubation period, capturing the time between exposure to the pathogen and the onset of infectiousness. This modification aims to provide a more realistic representation of the disease dynamics,

considering the latent period during which individuals are exposed but not yet infectious. The primary objective of this project is to introduce the Exposed compartment and then perform a stability analysis on the extended SEIR model. Stability analysis is a crucial step in understanding the long-term behavior of the system and assessing the effectiveness of control measures. By investigating the stability properties of the model, insights into the potential for disease persistence or fade-out can be gained, guiding public health interventions and policy recommendations. The subsequent sections of this report will delve into the details of the SEIR model and the stability analysis. Optimal control strategies for preventing the spread of listeriosis include treatment, vaccination, education, media campaigns, and the removal of contaminated food products. Treatment of infected humans and animals is found to be the most effective intervention strategy. Vaccination and education of susceptible humans can also help in curbing the disease. Media campaigns play a crucial role in raising awareness and reducing the exposure rate of humans by *Listeria*, leading to fewer infections and disease eradication. In preventing the transmission of listeriosis, removal rate of contaminated food products play very important. Implementing these control measures consistently and throughout the modeling time is recommended for better efficacy in controlling and reducing the disease. Infectious human listeriosis is a disease transmitted by animals too with a low occurrence rate but a high fatality rate among infected individuals globally [6]. Developing tactics to counter any disease outbreak is necessary since the disease is a major public health risk. When humans consume food products contaminated with *Listeria* or come into contact with the pathogen *Listeria monocytogenes* (*L. monocytogenes*) as a result of poor hygiene, they can become sick with Listeriosis. [8]; [7]. Laboratory-verified cases give the active bodies in charge of food-borne disease surveillance the information required for the diagnosis of human listeriosis, such as the World Health Organization [8], the Centers for Disease Control [9], and the National Institute of Communicable Disease (NICD) in South Africa. A bacterial culture obtained from biomedical tissues or fluids, such as spinal fluid, the placenta, or blood, is typically used to diagnose listeriosis [9]. The incubation period is one to twenty-one days, however in certain cases, the diagnosis may not come about for up to ninety days following the initial bacterial contact [9].

Headache, common flu-like symptoms, diarrhea, nausea, exhaustion, fever, loss of balance, stiff neck, convulsion and muscle aches are some of the signs and symptoms of infection. Moreover, it can result in early births, stillbirths, miscarriages, or potentially fatal infections for the fetus in pregnant women. Human listeria infections Almudena and Payeras-Cifre can be effectively treated with the ampicillin, A-lactam antibiotic [10]. Therefore, in case of an epidemic, specific precautionary measures can be implemented to control the disease, such as not to use contaminated food products, enforcing proper hygiene among manufacturing workers, and launching awareness campaigns. Offering a theoretical framework that allows variables influencing the viruses' control and transmission to be explicitly taken into account, mathematical models enhance our knowledge of pathogen dynamics [11]. The goal of disease epidemic modeling is to give strategies intended to stop the development of disease outbreaks a sound foundation. This comprises realistic, ideal approaches in models that enable evaluation of the measures implemented by public health authorities. The transmission dynamics of listeriosis have recently been studied using mathematical models (for instance in [1–5]). This study investigated the most effective management of listeriosis using a series of equations (mathematical model) that explained the spread of the sickness in throughout human and animal populations. Additionally, neither of these models take into account the scenario of the most effective approaches to prevent Listeriosis in humans by reducing the consumption of contaminated packaged foods food items. This work intends to establish and assess an appropriate control model for listeriosis, disease resulting from packaged food products with contamination. The best control measures to take are immune system stimulation, educational initiatives, and product recalls due to contamination.

The population increase is one of the many reasons why man has failed to preserve the natural environment. There are numerous detrimental effects of environmental degradation on humanity. As a result, it is now impossible to stop the spread of illness in society, particularly zoonotic illnesses like listeriosis [19]. The bacteria *Listeria monocytogenes* (*L. monocytogenes*) in food can cause listeriosis. *Listeria*-contaminated food can be the source of *L. monocytogenes* infections, but it can also be passed from mother to child through the skin or respiratory system during childbirth. *L. monocytogenes* can cause early deliveries, stillbirths, miscarriages, and potentially fatal illnesses in unborn children. *L. monocytogenes* is thought to be one of the main causes of bacterial meningitis in new borns. According to [20], cirrhosis, inadequate immune suppression, renal failure and diabetes, are a few of the conditions known to be associated with this illness. Payeras-Cifre and Ampicillin Almudena are examples of β -lactam antibiotics widely used for the treatment of human listeria infections. Although in the incidence of an epidemic, a few precautions can be im-

plemented to contain the outbreak, including the recall of contaminated food products, the practice of good hygiene by production workers, and the implementation of educational campaign programs. Because mathematical modeling produces insightful qualitative data, it has been shown to be an effective technique for monitoring and managing the propagation of numerous diseases. However, there exists a platform where the application of mathematical models is possible even in the absence of reliable data for data fitting. In [21], correspondent created a non-fractional An optimal control model is proposed to analyze the listeria infection dynamics in ready-to-eat food products (RTE) in order to investigate the disease's transmission dynamics. Their research suggested practical strategies to reduce the occurrence of listeriosis. The study in [22], Development of a system of model and analysis of equilibrium states and the anthrax-listeriosis co-infected model is used for sensitivity analysis. The study investigated a predictive modeling of listeriosis caused by cross-infection of prepared food items, in [23]. The findings indicated that reducing the quantity of workers with the infection and eliminating contaminated products would lower the total level of food contamination. A compartmental model of listeriosis including three humans and four animals was examined in the work in [24].

Qualitative analysis is done on the model's ability to maintain both endemic and disease-free equilibria as well as the potential for both forward and reverse bifurcation. Sensitivity analysis was employed to investigate the impact of altering the model parameters on the disease. The model includes education, immunization, and treatment of vulnerable (human) populations as dynamic control variable with time dependency. They devised the optimal course of action by further applying Pontryagin's Maximum Principle to the problem of listeriosis control. The model is numerically simulated, and the output is shown graphically and given a quantitative description. Prior to the work in [24], the authors in [25], focused on stability analysis when researching the listeria outbreaks in humans and animals. A deterministic co-infection model was constructed to describe the relationship between listeriosis and meningitis in [26]. We look at the meningitis and listeriosis only, sub-models. Each co-infection model and sub-model is examined mathematically. Characteristics of infection codynamics and severity are determined using Latin-hypercube sampling. According to numerical models, co-infections between listeriosis and meningitis are decreased when environmental pathogens causing the illness are reduced and meningitis recovery rates are raised. Additionally, in [27], created a mathematical modeling of listeriosis that took awareness campaigns into account. Study [28] examined the relationship between listeriosis and HIV/AIDS. They said the study will support the current endeavor to end the co-dynamics of HIV/AIDS and Listeria. In order to effectively control anthrax [29], conducted a sensitivity, bifurcation and study of modeling of co-dynamics of anthrax-Listeriosis with optimal control. They found that integrating anthrax and Listeriosis intervention techniques is required. In [30], they created a uniform perturbation of homotopy approach is proposed for the mathematical modeling of anthrax and listeriosis infections, taking to consideration the existing mathematical models. Models and simulation results can both have analytical solutions found using the homotopy perturbation technique (HPM). On the other hand, it is widely known that memory is crucial for the regulation of bodily functions and diseases ([31–39, 49–52]). Consequently, fractional calculus aids in the correct prediction of real-world phenomena by capturing these memory features. Worldwide interest in calculus of fractional and the examples shows it has increased recently. Numerous operators with fractional having distinct characteristics were developed and used to in daily life issues; refer to [40–44]. A fractional dynamics approach is used to investigate the interactions between nonsingular Mittag Leffler and coinfection of anthrax-listeriosis, this law was investigated by [45]. In [46], study investigated a listeriosis disease model using a fractal-fractional derivative in the Atangana-Beleanu-Caputo derivative (ABC) and Caputo. Researchers [12–18] found that the the Caputo fractal-fractional derivative fell short of ABC fractal-fractional derivative.

The remainder of manuscript is structured as follows: the mathematical model and its underlying assumptions are formulated in the following section. The features and analysis of the model without controls are presented in Section 3. The specification of acceptable optimal controls and the matching optimality system are provided in Section 4. Section 5 presents the results of numerical simulation, and Section 6 wraps up the investigation.

2. Framework of the Mathematical Model

The theoretical framework of our model encapsulates three interconnected components: the population of human, Processed edible food items, and the environmental presence of *Listeria monocytogenes* bacteria. Within the context of epidemiology, we categorize the population of human four distinct classes at any given time t : (i) Susceptible to infection ($S(t)$), (ii) Exposed but not yet infectious ($E(t)$), (iii) infection ($I(t)$), (iv) Actively carrying the *L. monocytogenes*, (v) Those who have successfully recovered ($R(t)$). This model is an expansion of the SEIR paradigm specifically designed to better understand the dynamic interactions within this system. Expressed mathematically, ($N(t)$) is the combined number of the four classes of the human population.

$$N(t) = S(t) + E(t) + I(t) + R(t) \quad (2.1)$$

Non-negative constant parameters N , μ_h , Λ_h , ρ_h , γ_l , κ_m , α , μ_f and Λ_f are introduced. The parameter N symbolizes the entire population in the disease-free state, namely at disease-free equilibrium i.e. at disease-free equilibrium. μ_h represents the mortality rate. The death rate caused by diseases multiplies the respective rates of the I classes S , E , R , and I respective rates of recovery due to death are $\mu_h S$, $\mu_h E$, $\mu_h R$, and $(\mu_h + \delta)I$ respectively. The rate of growth of susceptible humans is directly proportional to the number of the population of all the humans, $\mu_h N(t)$ and α denotes the rate at which population get recovered from the disease. Susceptible individuals become infected through the ingestion of contaminated food and exposure to *Listeria* in the environment. This infection rate, denoted as Λ_h , is determined by the formula $\Lambda_h = F_c \omega_1 + L_m \omega_2$, where ω_1 and ω_2 represent the effective contact rates (exposure to bacteria refer to the contacts that will lead to infections) for the humans in the susceptible compartment and *L. monocytogenes* respectively. $0 \leq \kappa_m \leq 1$ is carrying capacity of *Listeria monocytogene* whose net growth rate is r_l and denoted by L_m . Food products can be classified into two groups: free from contamination that is uncontaminated F_u , and contaminated food products F_c , with $F = F_u + F_c$ section of total food items. Once susceptibles are infected, they become infectious and move to compartment I . Infectives move to compartment R with a recovery rate α , recovered persons can be susceptibility again at a rate ρ_h . We also have the following assumptions: (i) The bacteria grow logistically such that: $\frac{dL_m}{dt} = r_l \cdot L_m \cdot \left(1 - \frac{L_m}{\kappa_m}\right)$. (ii) μ_f is productivity rate of pure food, the productivity assumed to yield pure food (food without contamination). The contamination rate of pure food is Λ_f caused by the bacterial environment and the contamination of food during the handling and distribution operations of the factory. i.e., $\Lambda_f = \omega_2 L_m + \omega_3 F_c$. where ω_3 represents effective contact rate of the contamination of pure food items caused by bacterium. (iii) All food under the control of removal rate μ_f . (iv) The rate at which individuals move from Exposed to Infected compartment is γ_e . With the above parameters and assumptions, the pictorial representation of the model and mathematical is as follows and the model is represented by equations given below:

The following set of ordinary differential equations governs our enhanced paradigm.

$$\left\{ \begin{array}{l} \frac{dS}{dt} = \mu_h N + \rho_h R - (\Lambda_h + \mu_h) S \\ \frac{dE}{dt} = \Lambda_h S - (\gamma + \mu_h) E \\ \frac{dI}{dt} = \gamma E - (\alpha + \mu_h) I \\ \frac{dR}{dt} = \alpha I - (\rho_h + \mu_h) R \\ \frac{dL_m}{dt} = r_l L_m \left(1 - \frac{L_m}{\kappa_m}\right) \\ \frac{dF_u}{dt} = \mu_f F - (\Lambda_f + \mu_f) F_u \\ \frac{dF_c}{dt} = \Lambda_f F_u - \mu_f F_c \end{array} \right. \quad (2.2)$$

We substitute $R(t) = N(t) - S(t) - E(t) - I(t)$ from (1), we convert equation (1) into a dimensionless system by

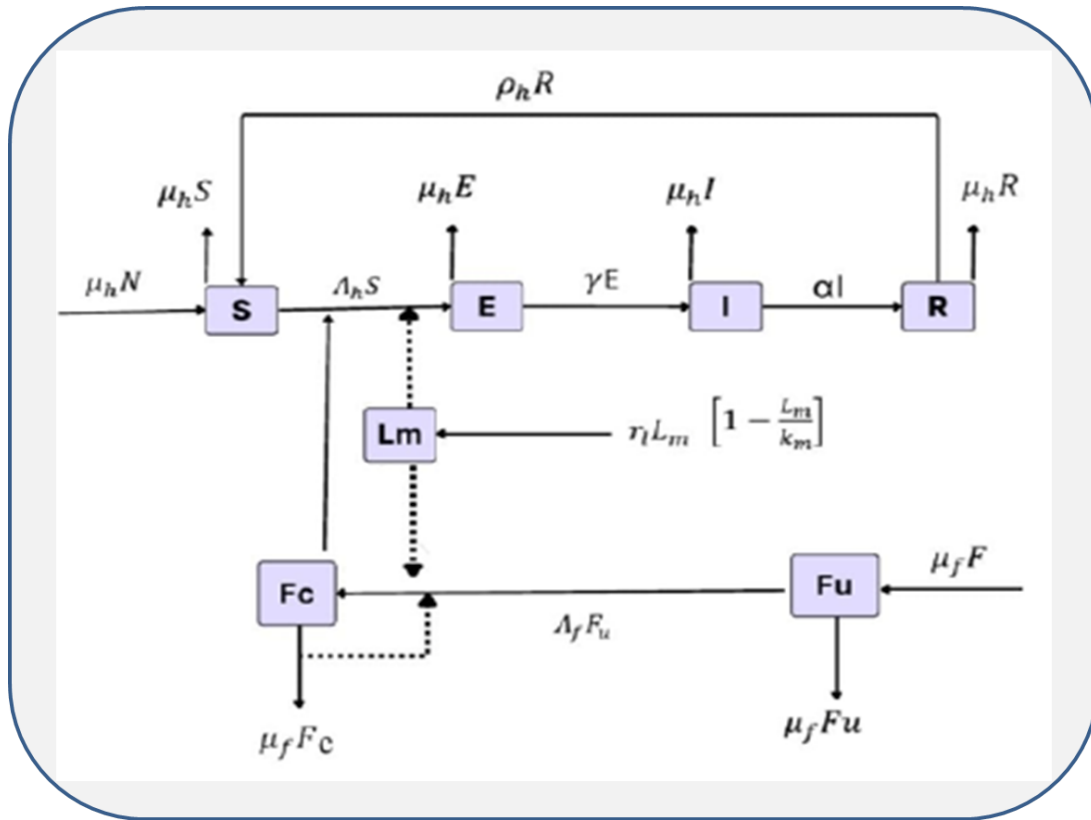


Figure A: Schematic diagram of the model

establishing a certain condition $s = \frac{S}{N}$, $e = \frac{E}{N}$, $i = \frac{I}{N}$, $l_m = \frac{L_m}{\kappa_m}$, $f_u = \frac{F_u}{F}$, and $f_c = \frac{F_c}{F}$. The resulting equations are:

$$\left\{ \begin{array}{l} \frac{ds}{dt} = \mu_h + \rho_h(1 - s - e - i) - (\tilde{\Lambda}_h + \mu_h)s \\ \frac{de}{dt} = \tilde{\Lambda}_h s - (\gamma + \mu_h)e \\ \frac{di}{dt} = \gamma e - (\alpha + \mu_h)i \\ \frac{dl_m}{dt} = r_l l_m (1 - l_m) \\ \frac{df_u}{dt} = \mu_f - (\tilde{\Lambda}_f + \mu_f)f_u \\ \frac{df_c}{dt} = \tilde{\Lambda}_f f_u - \mu_f f_c \end{array} \right. \quad (2.3)$$

where $\tilde{\Lambda}_h = \omega_1 f_c + \omega_2 l_m$ and $\tilde{\Lambda}_f = \omega_2 l_m + \omega_3 f_c$. The system of equations (3) is non-negative initial conditions, provided

$$s(0) > 0, e(0) \geq 0, i(0) \geq 0, l_m(0) \geq 0, f_u(0) \geq 0, f_c(0) \geq 0. \quad (2.4)$$

3. Model Analysis

3.1. Positivity and Boundedness of Solutions

Here, we demonstrate the condition of existence, non-negativeness, and boundedness of the solutions for equations (3) within a specific region Ω contained in \mathbb{R}_+^6 . The theorem given below allows to establish the positivity of the solutions.

Theorem 3.1. *All the solutions of the system (3) is contained in the region $\Omega \in \mathbb{R}_+^6$ for the initial conditions (4) in Ω , where Ω is*

$$\Omega = \{(s, e, i, l_m, f_c, f_u) \in \mathbb{R}_+^6 : 0 \leq s + e + i \leq 1, 0 \leq f_u + f_c \leq 1, 0 \leq l_m \leq 1, \}$$

proof: The differential inequality provides the overall change in the human population as expressed by the initial two equations of system (3).

$$\frac{dn}{dt} \leq (1 - s - e - i)(\mu_h + \rho_h) \quad (3.1)$$

for value of $n = s + i \leq 1$ and using $\Phi_0 = s + e + i$, which have

$$\Phi_0(t) = 1 - \frac{\Phi_0(0)}{e^{(\mu_h + \rho_h)t}}$$

Given that $\Phi_0(0) \leq 1$, the upper bound of $\Phi_0(t)$ is 1, as $\lim_{t \rightarrow \infty} \Phi_0(t) = 0$. We now examine the bacterial population in the environment, as represented by the equation:

$$\frac{dl_m}{dt} = r_l l_m (1 - l_m) \quad (3.2)$$

Solving this first order equation, we get

$$l_m(t) = \frac{1}{1 + \Phi_1 e^{-r_1 t}}$$

where Φ_1 is a constant. Therefore, the value of $l_m(t)$ ranges from $[0, 1]$. This signifies that the growth of the L. monocytogene is bounded. Now, we shall consider the rate of change in quantity of total prepared food products both contaminated and uncontaminated from the equations of system (3), is

$$\frac{df}{dt} = \mu_f (1 - f)$$

whose solution is given by

$$f(t) = 1 - \frac{\Phi_2}{e^{(\mu_f)t}}$$

where Φ_2 is a constant and $\lim_{t \rightarrow \infty} f(t)$ tends to 1. So existence and boundedness of the solution be in domain Ω for $t > \infty$.

Theorem 3.2. For each non-negative parameter initial condition $(s_0, e_0, i_0, l_{m0}, f_{u0}, f_{c0})$ as given in (4), For $t \geq 0$, all results of system (3), $((s(t), e(t), i(t), l_m(t), f_u(t), f_c(t)))$, are non-negative.

As time t increases indefinitely, for any $t \geq 0$ the set (3) of differential equation remain non-negative; that is, $s(t) > 0$, $e(t) > 0$, $i(t) > 0$, $f_u(t) > 0$, $l_m(t) > 0$ and $f_c(t) > 0$.

3.2. Stability Analysis

Equating set (3) of equation to zero allows us for determining the stable states.

$$\mu_h + \rho_h(1 - s^* - e^* - i^*) - (\mu_h + \omega_1 f_c + \omega_2 l_m) s^* = 0, \quad (3.3)$$

$$(\omega_1 f_c + \omega_2 l_m) s^* - (\gamma + \mu_h) e^* = 0, \quad (3.4)$$

$$\gamma e^* - (\alpha + \mu_h) i^* = 0. \quad (3.5)$$

$$(r_l) l_m^* (1 - l_m^*) = 0, \quad (3.6)$$

$$\mu_f - f_u^* (\omega_2 l_m^* + \omega_3 f_c^* + \mu_f) = 0, \quad (3.7)$$

$$(\omega_2 l_m^* + \omega_3 f_c^*) f_u^* - \mu_f f_c^* = 0. \quad (3.8)$$

We shall now solve these system of equations. Solving equation (10), we get two solutions

$$l_{m0}^* = 0 \quad \text{or} \quad l_{m1}^* = 1.$$

Substitute $l_{m0}^* = 0$ into Equation (11), we solve for f_c^* and f_u^* and we get,

$$f_u^* = \frac{\mu_f}{\mu_f + \omega_3 f_c^*} \quad \text{and} \quad f_c^* = \frac{\mu_f}{\omega_3} \left(\frac{1}{f_u^*} - 1 \right)$$

Substitute the value of f_u^* into equation (12), we get

$$\omega_3 \mu_f f_c^* - \mu_f f_c^* (\omega_3 f_c^* + \mu_f) = 0$$

Solving this equation for f_c^* , we get

$$f_{c0}^* = 0 \quad \text{or} \quad f_{c1}^* = \frac{\omega_3 - \mu_f}{\omega_3}$$

From our assumptions, we have defined μ_f as the production rate of uncontaminated food. Now, we will define two new parameters: $\Psi_0 = \frac{\mu_f}{\omega_3}$ and $\Re_f = \frac{\omega_3}{\mu_f}$

\mathfrak{R}_f connotes the Basic reproduction number \mathfrak{R}_0 . This suggests the average proportion of food items that can be infected which gives rise to the occurrence of human Listeria infections. Substituting these two values into the formula for $f_{c_1}^*$, we get $f_{c_1}^* = \Psi_0(\mathfrak{R}_f - 1)$

Theorem 3.3. *There exist steady state $f_{c_1}^*$ whenever $\mathfrak{R}_f > 1$.*

If $l_{m_0}^* = 0$, then $f_{c_0}^* = 0$. Therefore, $f_u^* = 1$, $\tilde{\Lambda}_h = 0$ and $\tilde{\Lambda}_f = 0$. At the Disease-Free Equilibrium, the number of individuals in the infected/infectious and exposed compartment is zero $e^* = i^* = 0$. This implies that there are no actively infected individuals in the population, and the disease is not spreading. The entire population is typically in the susceptible compartment $s^* = 1$, indicating that everyone is susceptible to the disease but not currently infected. the Disease-Free Equilibrium is determined by setting the equations governing the dynamics of the system to values that result in zero infections. This often involves setting the initial conditions or specific parameters such that the rate of infection becomes zero. The Disease-Free Equilibrium State will be given by

$$\mathfrak{E}^* = (s^*, e^*, i^*, l_{m_0}^*, f_u^*, f_{c_0}^*) = (1, 0, 0, 0, 1, 0)$$

3.2.1. Local Stability of \mathfrak{E}^*

Theorem 3.4. *Local asymptotically stability of the disease free system of model (3) provided $r_l > 0$ and $\mathfrak{R}_f < 1$ if not unstable.*

The linearized form of the set (3) of equations at \mathfrak{E}^* is

$$J(\mathfrak{E}^*) = \begin{bmatrix} -(\rho_h + \tilde{\Lambda}_h + \mu_h) & -\rho_h & -\rho_h & 0 & 0 & 0 \\ \tilde{\Lambda}_h & -(\gamma + \mu_h) & 0 & 0 & 0 & 0 \\ 0 & \gamma & -(\alpha + \mu_h) & 0 & 0 & 0 \\ 0 & 0 & 0 & r_l & 0 & 0 \\ 0 & 0 & 0 & 0 & -(\tilde{\Lambda}_f + \mu_f) & 0 \\ 0 & 0 & 0 & 0 & \tilde{\Lambda}_f & -\mu_f \end{bmatrix}$$

Calculation of Eigenvalues:

$$\begin{aligned} \lambda_1 &= r_l \\ \lambda_2 &= -\mu_f \\ \lambda_3 &= -\gamma - \mu_h \\ \lambda_4 &= -\alpha - \mu_h \\ \lambda_5 &= -\mu_h - \rho_h \\ \lambda_6 &= -\mu_f + \omega_3 = \mu_f(\mathfrak{R}_f - 1) \end{aligned}$$

Analysis: The parameters α , γ , r_l , μ_f , μ_h and ρ_h are **all non-negative**: (i) whenever $\mathfrak{R}_f < 1$, then $\lambda_6 < 0$. (ii) whenever $r_l > 0$, then all six of the characteristics root at \mathfrak{E}^* will be negative. In this case, \mathfrak{E}^* is **Asymptotically Stable**. However, if $r_l > 0$, then atleast one of the eigenvalues λ_1 is positive irrespective of the value of \mathfrak{R}_f and λ_6 . Therefore, steady state \mathfrak{E}^* is Unstable. The biological meaning of $r_l < 0$ is pointing to the declining the growth rate

of Listeria population, indicating a decline towards its maximum limit. This observation aligns with logistic growth dynamics. We know that $l_{m_0}^* = 0$ and $f_{c_1} = \Psi_0 (\mathfrak{R}_f - 1)$, substituting these values into (7) and (8), we get,

$$\mu_h + \rho_h(1 - s^* - e^* - i^*) - (\mathcal{A}_0)s^* = 0 \quad (3.9)$$

$$\omega_1 \Psi_0 (\mathfrak{R}_f - 1)s^* - (\gamma + \mu_h)e^* = 0 \quad (3.10)$$

Assuming $\mathcal{A}_0 = \mu_h + (\mathfrak{R}_f - 1)\omega_1 \Psi_0$, from (7) and (8) simultaneously for s^* and e^* by taking $i^* = 0$, we get

$$e^* = \frac{(\mu_h + \rho_h)(\mathfrak{R}_f - 1)\omega_1 \psi_0}{\mathcal{A}_1 + (\gamma + \mu_h + \rho_h)\omega_1 \Psi_0 (\mathfrak{R}_f - 1)}$$

$$s^* = \frac{(\mu_h + \rho_h)(\gamma + \mu_h)}{\mathcal{A}_1 + (\gamma + \mu_h + \rho_h)\omega_1 \Psi_0 (\mathfrak{R}_f - 1)}$$

Assuming $\mathcal{A}_1 = (\gamma + \mu_h)(\rho_h + \mu_h)$

3.2.2. Listerosis-Free State and Local Stability of \mathfrak{E}^{**}

We shall denote a Listerosis-Free State (LFS) using $\mathfrak{E}^{**} = (s^{**}, e^{**}, i^{**}, l_{m_0}^{**}, f_u^{**}, f_{c_1}^{**})$, where

$$e^{**} = \frac{(\mu_h + \rho_h)(\mathfrak{R}_f - 1)\omega_1 \psi_0}{\mathcal{A}_1 + (\gamma + \rho_h + \mu_h)(\mathfrak{R}_f - 1)\omega_1 \Psi_0}$$

$$s^{**} = \frac{(\gamma + \mu_h)(\mu_h + \rho_h)}{\mathcal{A}_1 + (\gamma + \rho_h + \mu_h)(\mathfrak{R}_f - 1)\omega_1 \Psi_0}$$

$$l_{m_0}^{**} = 0$$

$$f_u^{**} = \frac{1}{1 + (\mathfrak{R}_f - 1)\mathfrak{R}_e}$$

$$f_{c_1}^{**} = \Psi_0 (\mathfrak{R}_f - 1)$$

with $\mathfrak{R}_e = \frac{\omega_3}{\omega_2}$

As we asserted previously in the existence of \mathfrak{E}^* , the existence of \mathfrak{E}^{**} is also subject to $\mathfrak{R}_f > 1$

Theorem 3.5. *The Listeriosis-Free State of model system (3) have local asymptotic stability when $r_l > 0$ and $\mathfrak{R}_f > 1$, and is unstable otherwise.*

The linearized form of the set (3) of equations

$$J(\mathfrak{E}^{**}) = \begin{bmatrix} -Q_0 & -\rho_h & -\rho_h & -\omega_2 \tilde{s}^{**} & 0 & -\omega_1 \tilde{s}^{**} \\ \omega_1 \tilde{f}_c^{**} & -Q_1 & 0 & \omega_2 \tilde{s}^{**} & 0 & \omega_1 \tilde{s}^{**} \\ 0 & \gamma & -Q_2 & 0 & 0 & 0 \\ 0 & 0 & 0 & r_l & 0 & 0 \\ 0 & 0 & 0 & -\omega_2 \tilde{f}_u^{**} & -Q_3 & -\omega_3 \tilde{f}_u^{**} \\ 0 & 0 & 0 & \omega_2 \tilde{f}_u^{**} & \omega_3 \tilde{f}_c^{**} & Q_4 \end{bmatrix}$$

We can proceed by ignoring the Infected compartment and reducing the matrix to

$$\begin{bmatrix} -Q_0 & -\rho_h & -\omega_2 \tilde{s}^{**} & 0 & -\omega_1 \tilde{s}^{**} \\ \omega_1 \tilde{f}_c^{**} & -Q_1 & \omega_2 \tilde{s}^{**} & 0 & \omega_1 \tilde{s}^{**} \\ 0 & 0 & r_l & 0 & 0 \\ 0 & 0 & -\omega_2 \tilde{f}_u^{**} & -Q_3 & -\omega_3 \tilde{f}_u^{**} \\ 0 & 0 & \omega_2 \tilde{f}_u^{**} & \omega_3 \tilde{f}_c^{**} & Q_4 \end{bmatrix}$$

where

$$\begin{aligned} Q_0 &= \rho_h + \mu_h + \omega_1 \tilde{f}_c^{**} \\ Q_1 &= \gamma + \mu_h \\ Q_2 &= \alpha + \mu_h \\ Q_3 &= \mu_f + \omega_3 \tilde{f}_c^{**} \\ Q_4 &= \omega_3 \tilde{f}_u^{**} - \mu_f \end{aligned}$$

From the above linearised matrix, we get the eigenvalues by finding the determinants of these two matrices :

$$J_1(\mathfrak{E}^{**}) = \begin{vmatrix} -Q_0 & -\rho_h \\ \omega_1 \Psi_0(\mathfrak{R}_f - 1) & -Q_1 \end{vmatrix}$$

$$\text{and } J_2(\mathfrak{E}^{**}) = \begin{vmatrix} -Q_3 & -\frac{\omega_3}{1 + \mathfrak{R}_e(\mathfrak{R}_f - 1)} \\ \omega_3 \Psi_0(\mathfrak{R}_f - 1) & \frac{\omega_3}{1 + \mathfrak{R}_e(\mathfrak{R}_f - 1)} - \mu_f \end{vmatrix}$$

The solutions of these can be derived from the solutions of the characteristic equations

$$\begin{aligned} \Lambda^2 + \zeta_4 \Lambda + \zeta_3 &= 0 \\ \Lambda^2 + \zeta_6 \Lambda + \zeta_5 &= 0 \end{aligned} \tag{3.11}$$

$$\begin{aligned} \zeta_1 &= r_l \\ \zeta_2 &= -\mu_f \\ \zeta_3 &= (\mu_h + \rho_h)(\alpha + \mu_h) + (\gamma + \mu_h + \rho_h)(\mathfrak{R}_f - 1)\omega_1 \Psi_0 \\ \zeta_4 &= \alpha + 2\mu_h + (\mathfrak{R}_f - 1)\omega_1 \Psi_0 + \rho_h \\ \zeta_5 &= \frac{(\mu_f(1 + (\mathfrak{R}_f - 1)\mathfrak{R}_e)\mu_f + \omega_3 \Psi_1)}{1 + (\mathfrak{R}_f - 1)\mathfrak{R}_e} \\ \zeta_6 &= \frac{2\mu_f(1 + (\mathfrak{R}_f - 1)\mathfrak{R}_e) + \omega_3 \Psi_1}{1 + (\mathfrak{R}_f - 1)\mathfrak{R}_e} \end{aligned}$$

Defined $\Psi_1 = ((1 + \mathfrak{R}_e(\mathfrak{R}_f - 1))(\mathfrak{R}_f - 1)\Psi_0 - 1)$. The Routh-Hurwitz stability criterion states that the values of $\zeta_3, \zeta_4, \zeta_5$ and ζ_6 will be positive when the value of $R_f > 1$. It can be concluded that quadratic equation (15) have those characteristic values which possess real part as negative. Therefore $J_2(\mathfrak{E}^{**})$ will be asymptotically stable if and only if $r_l > 0$. If $r_l < 0$, then we will get unstable state of $J_2(\mathfrak{E}^{**})$. Therefore, we have that all the results of the

two quadratic equations or of the two quadratic equations or the characteristic root of the matrix of linearized form which contains real part negative. As we have established before, all of the parameters are non-negative, therefore ζ_2 , is always negative and if $\Re_f > 1$, then $\zeta_3, \zeta_4, \zeta_5, \zeta_6$, will be positive. Therefore, \mathfrak{E}^{**} exhibits local asymptotic stability if and only if r_1 , is negative, meaning $\zeta_1 < 0$, as all the characteristic root will be negative. However, if r_1 is positive, meaning $\zeta_1 > 0$, then \mathfrak{E}^{**} , is in unstable steady state. Now, we shall consider the case of $l_{m_1}^{**} = 1$, substituting this value in equation (11), we get,

$$f_u^* = \frac{\mu_f}{\omega_2 + \omega_3 f_c^* + \mu_f}$$

substituting this value into equation (12), we get $C_1 f_c^{*2} + C_2 f_c^* + C_3 = 0$. Where $C_1 = \omega_3 \mu_f < 0$ $C_2 = \omega_2 \mu_f - (\frac{1}{\Re_f} - 1)$ $C_3 = -\omega_2 \mu_f > 0$. we can predict that $C_2 < 0$ if $\Re_f < 1$ and $C_2 < 0$ if $\Re_f < 1$. Therefore, regardless of the numerical value of C_1 , the quadratic equation in f_c^* will always have a positive characteristic root, say f_{c1}^* and taking $l_{m_1}^{**} = 1$ in equations (7) and (8), the equations transform to

$$\begin{aligned} \mu_h + \rho_h(1 - s^* - e^* - i^*) - (\mu_h + \omega_1 \tilde{f}_c^* + \omega_2)s^* &= 0 \\ (\omega_1 \tilde{f}_c^* + \omega_2)s^* - (\gamma + \mu_h)e^* &= 0 \end{aligned}$$

Solving these two equations simultaneously for s^* and e^* by taking $i^* = 0$, we get

$$\begin{aligned} s^* &= \frac{(\gamma + \mu_h)(\mu_h + \rho_h)}{\mu_h^2 + \gamma(\omega_2 + \omega_1 \tilde{f}_c^*) + \rho_h \Gamma_0 + \mu_h \Gamma_1} \\ e^* &= \frac{(\mu_h + \rho_h)(\omega_2 + \omega_1 \tilde{f}_c^*)}{\mu_h^2 + \gamma(\omega_2 + \omega_1 \tilde{f}_c^*) + \rho_h \Gamma_0 + \mu_h \Gamma_1} \end{aligned}$$

where $\Gamma_0 = (\gamma + \omega_2 + \omega_1 \tilde{f}_c^*)$ and $\Gamma_1 = (\rho_h + \gamma + \omega_2 + \omega_1 \tilde{f}_c^*)$

3.3. Listeriosis Endemic State \mathfrak{E}^{***}

An endemic state of listeriosis refers to a persistent, often stable, presence of the disease within a population over an extended period. Unlike the disease-free equilibrium, which represents a state where the infection has been eradicated, an endemic state suggests that the infection continues to circulate within the population, and new cases may occur regularly. In the context of mathematical modeling and epidemiology, an endemic equilibrium is reached when the number of new infections and recoveries balance out, leading to a stable level of disease prevalence. This equilibrium is characterized by a non-zero, steady-state level of infected individuals in the population. The Listeriosis Endemic State (LES) is represented by $\mathfrak{E}^{***} = (\tilde{s}^{***}, \tilde{e}^{***}, \tilde{i}^{***}, \tilde{l}_{m_1}^{***}, \tilde{f}_u^{***})$ and given by

$$\tilde{s}^{***} = \frac{(\mu_h + \rho_h)(\gamma + \mu_h)}{\mathcal{A}_2 + \rho_h \Gamma_0 + \mu_h \Gamma_1} \quad \tilde{e}^{***} = \frac{(\omega_2 + \omega_1 \tilde{f}_c^*)(\mu_h + \rho_h)}{\mathcal{A}_2 + \rho_h \Gamma_0 + \mu_h \Gamma_1}$$

$$\tilde{l}_{m_1}^{***} = \tilde{f}_u^{***} = \frac{1}{1 + \frac{\omega_2}{\mu_f} + \tilde{f}_c^* \Re_f}$$

where $\mathcal{A}_2 = \mu_h^2 + \gamma(\omega_2 + \omega_1 \tilde{f}_c^*)$

3.3.1. Local Stability of \mathfrak{E}^{***}

Theorem 3.6. *The set (3) of equations exhibits local asymptotic stability for the Listeriosis Endemic state when the value of $\mathfrak{R}_f > 1$, and unstable elsewhere.*

The linearized form of the set (3) of equations at \mathfrak{E}^{***} is

$$J(\mathfrak{E}^{***}) = \begin{bmatrix} -Q_5 & -\rho_h & -\rho_h & -\omega_2 \tilde{s}^{***} & 0 & -\omega_1 \tilde{s}^{***} \\ Q_6 & -Q_7 & 0 & \omega_2 \tilde{s}^{***} & 0 & \omega_1 \tilde{s}^{***} \\ 0 & \gamma & -Q_8 & 0 & 0 & 0 \\ 0 & 0 & 0 & -r_l & 0 & 0 \\ 0 & 0 & 0 & -\omega_2 \tilde{f}_u^{***} & -Q_9 & -\omega_3 \tilde{f}_u^{***} \\ 0 & 0 & 0 & \omega_2 \tilde{f}_u^{***} & Q_{10} & Q_{11} \end{bmatrix}$$

where

$$\begin{aligned} Q_5 &= \rho_h + \mu_h + \omega_1 \tilde{f}_c^* + \omega_2 \\ Q_6 &= \omega_1 \tilde{f}_c^* + \omega_2 \\ Q_7 &= \gamma + \mu_h \\ Q_8 &= \alpha + \mu_h \\ Q_9 &= \mu_f + \omega_2 + \omega_3 \tilde{f}_c^* \\ Q_{10} &= \omega_2 + \omega_3 \tilde{f}_c^* \\ Q_{11} &= \omega_3 \tilde{f}_u^{***} - \mu_f \end{aligned}$$

We will reduce the linearised matrix by removing the infected compartment and deal with the susceptible and exposed compartment. The linearised matrix reduces to

$$\begin{bmatrix} -Q_5 & -\rho_h & -\omega_2 \tilde{s}^{***} & 0 & -\omega_1 \tilde{s}^{***} \\ Q_6 & -Q_7 & \omega_2 \tilde{s}^{***} & 0 & \omega_1 \tilde{s}^{***} \\ 0 & 0 & -r_l & 0 & 0 \\ 0 & 0 & -\omega_2 \tilde{f}_u^{***} & -Q_9 & -\omega_3 \tilde{f}_u^{***} \\ 0 & 0 & \omega_2 \tilde{f}_u^{***} & Q_{10} & Q_{11} \end{bmatrix}$$

The eigenvalues of this matrix are $\epsilon_1 = -r_l$ and the solutions to the characteristic polynomials obtained from

$\begin{vmatrix} -Q_5 & -\rho_h \\ Q_6 & -Q_7 \end{vmatrix}$ given by $\Lambda^2 + \epsilon_2 \Lambda + \epsilon_3 = 0$, where

$$\begin{aligned} \epsilon_2 &= \gamma + 2\mu_h + \rho_h + \omega_1 \tilde{f}_c^{***} + \omega_2 \\ \epsilon_3 &= \mu_h^2 + \gamma(\omega_2 + \omega_1 \tilde{f}_c^{***}) + \rho_h(\gamma + \omega_2 + \omega_1 \tilde{f}_c^{***}) + \mu_h(\gamma + \rho_h + \omega_2 + \omega_1 \tilde{f}_c^{***}) \end{aligned}$$

Both ϵ_2 and ϵ_3 are always positive. The remaining eigenvalues are calculated from the determinant $\begin{vmatrix} -Q_9 & -\omega_3 \tilde{f}_u^{***} \\ Q_{10} & -Q_{11} \end{vmatrix}$ given by $\Lambda^2 + \epsilon_4 \Lambda + \epsilon_5 = 0$, where

$$\epsilon_4 = \frac{\omega_2}{\omega_3} + (\tilde{f}_c^* - \tilde{f}_u^{***}) + \frac{2}{\Re_f}$$

$$\epsilon_5 = \frac{\omega_2}{\omega_3} + (\tilde{f}_c^* - \tilde{f}_u^{***}) + \frac{1}{\Re_f}$$

ϵ_4 and ϵ_5 are positive iff $\tilde{f}_c^* - \tilde{f}_u^{***} > 0$.

i.e ϵ_4 and ϵ_5 are positive if the value of \tilde{f}_c^* is greater than \tilde{f}_u^{***} . Based on the Routh Hurwitz stability criterion, it may be predicted that all the eigenvalues or solutions of the quadratic equations include negative real parts, similar to the previous case. The biological implication is that in order for the Listeriosis epidemic to reach the Listeriosis Endemic State, there must be a lesser number of uncontaminated food products compared to contaminated food products.

4. Computer and Numerical Simulations

In the corresponding sections, numerical simulations for the compartmental model are provided using the most relevant and well-fitting parameter values. Every visual projection has been positioned, styled, and presented in an eye-catching manner.

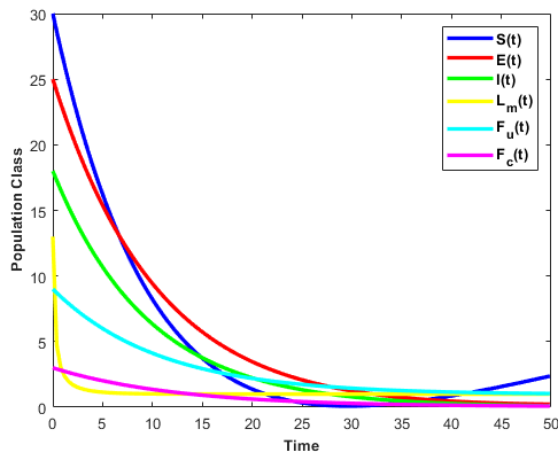


Fig. 1

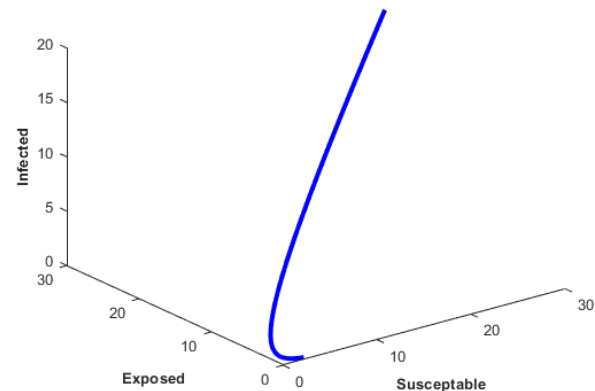


Fig. 2

Fig.1 Represents the time series evaluation of population classes and **Fig.2** Represents phase portrait of susceptible, exposed and infected populations with the attributes of $\mu_h = 0,1, \alpha = 0,0094, \rho_h = 0,09, r_l = 0,40, \omega_1 = 0,0380, \omega_2 = 0,0020, \omega_3 = 0,00050, \mu_f = 0,0076, \gamma_1 = 0,0035, \mu_f = 0,09, \lambda_h = 0,0056, \lambda_f = 0,0036$.

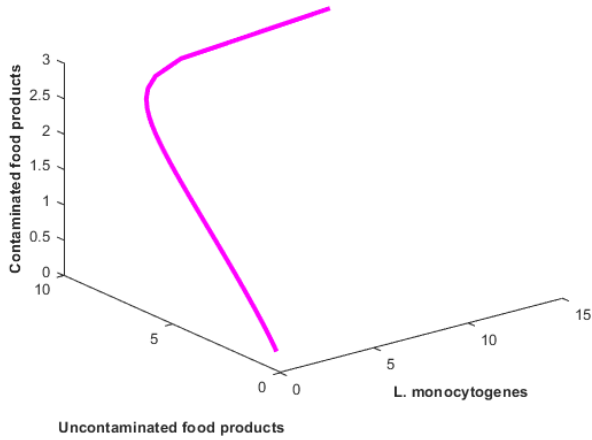


Fig. 3

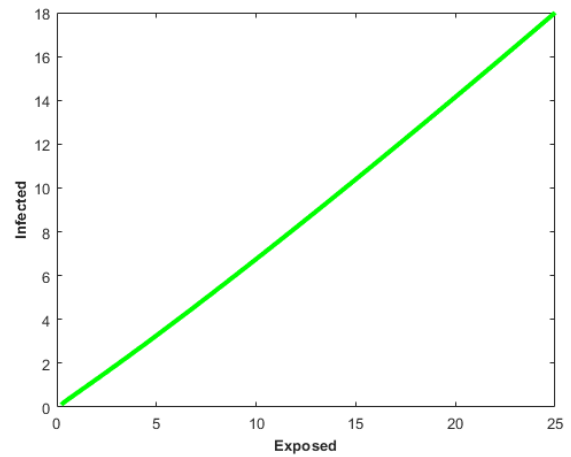


Fig. 4

Fig.3 represents the phase portrait of population classes L-Monocytogenes, uncontaminated food products, contaminated food products and **Fig.4** represents the variation of infected populations with reference to exposed populations with the attributes of $\mu_h = 0,1$, $\alpha = 0,0094$, $\rho_h = 0,09$, $r_l = 0,40$, $\omega_1 = 0,0380$, $\omega_2 = 0,0020$, $\omega_3 = 0,00050$, $\mu_f = 0,0076$, $\gamma_1 = 0,0035$, $\mu_h = 0,09$, $\lambda_h = 0,0056$, $\lambda_f = 0,0036$.

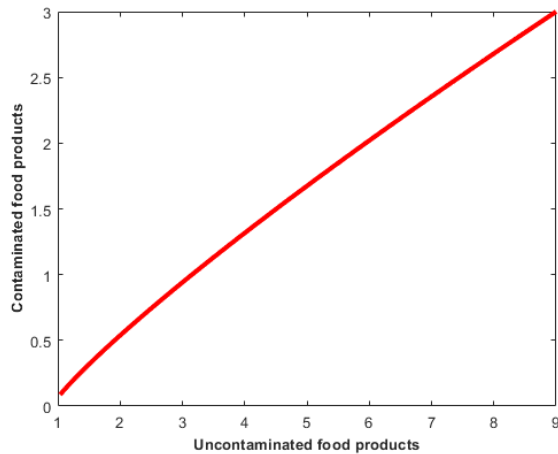


Fig. 5

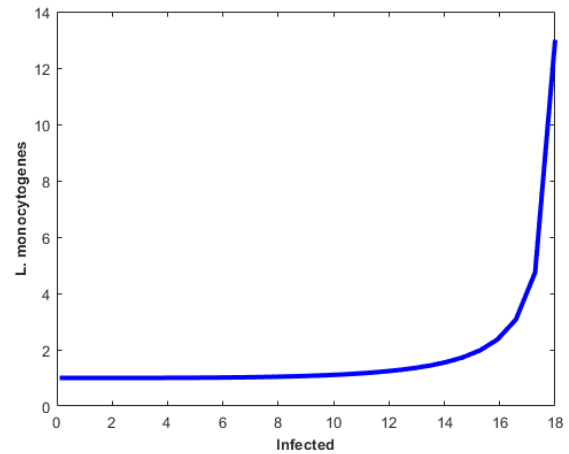


Fig. 6

Fig.5 Represents the variation of uncontaminated food products with reference to the contaminated food products and **Fig.6** Represents the variation of infected populations with reference to L.monocytogenes with the attributes of $\mu_h = 0,1, \alpha = 0,0094, \rho_h = 0,09, r_l = 0,40, \omega_1 = 0,0380, \omega_2 = 0,0020, \omega_3 = 0,00050, \mu_f = 0,0076, \gamma_1 = 0,0035, \mu_f = 0,09, \lambda_h = 0,0056, \lambda_f = 0,0036$.

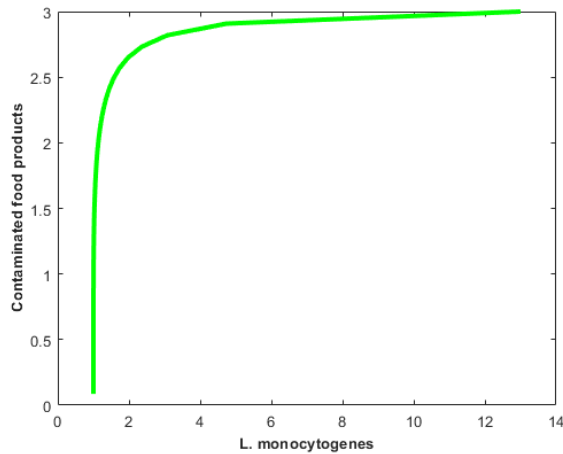


Fig. 7

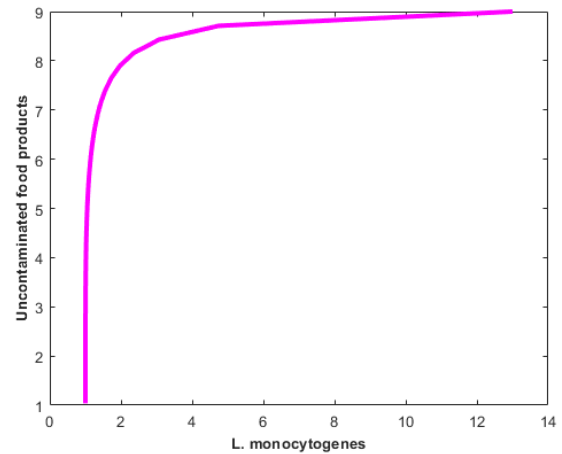


Fig. 8

Fig.7 Representing the variation of L.monocytogenes with reference to the contaminated food products and **Fig.8** Representing the variation of L.monocytogenes with reference to L.monocytogenes with the attributes of $\mu_h = 0,1, \alpha = 0,0094, \rho_h = 0,09, r_l = 0,40, \omega_1 = 0,0380, \omega_2 = 0,0020, \omega_3 = 0,00050, \mu_f = 0,0076, \gamma_1 = 0,0035, \mu_f = 0,09, \lambda_h = 0,0056, \lambda_f = 0,0036$.

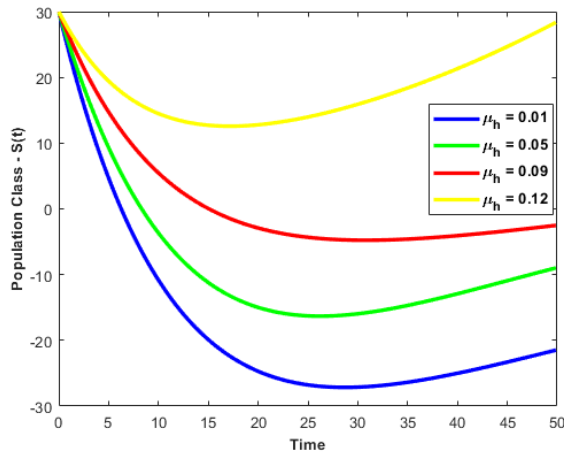


Fig. 9a

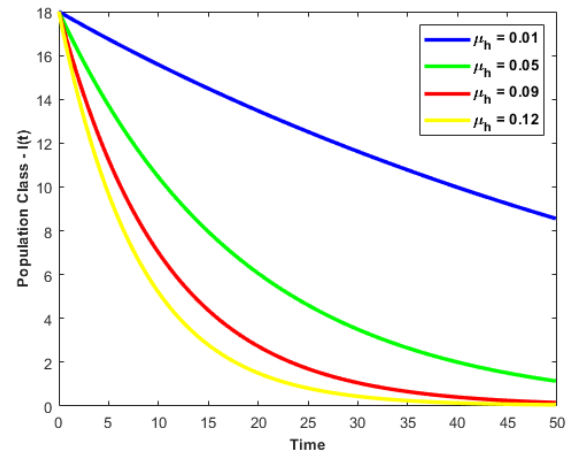


Fig. 9b

Fig.9a Evaluation of population density using time series analysis of $S(t)$ and **Fig.9b** Evaluation of population density using time series analysis of $I(t)$ as μ_h is increasing with the attributes of $\mu_h = 0,1, \alpha = 0,0094, \rho_h = 0,09, r_l = 0,40, \omega_1 = 0,0380, \omega_2 = 0,0020, \omega_3 = 0,00050, \mu_f = 0,0076, \gamma_1 = 0,0035, \mu_f = 0,09, \lambda_h = 0,0056, \lambda_f = 0,0036$.

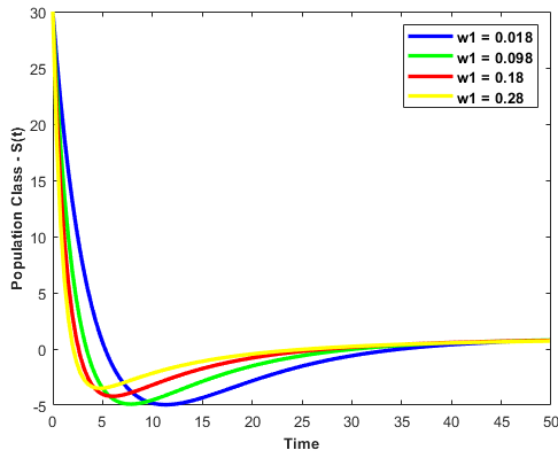


Fig. 10a

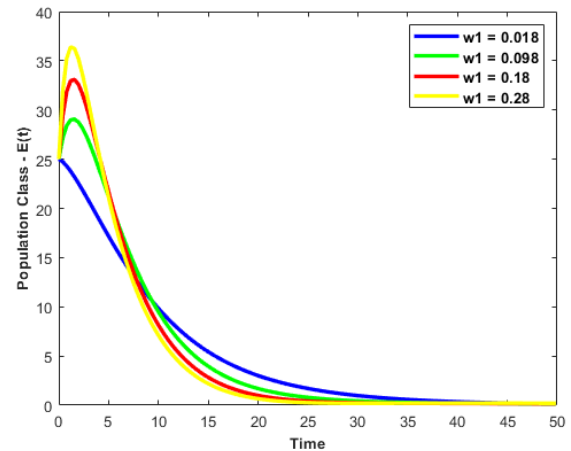


Fig. 10b

Fig.10a Evaluation of population density using time series analysis of $S(t)$ and **Fig.10b** Evaluation of population density using time series analysis of $E(t)$ as w_1 is increasing with the attributes of $\mu_h = 0,1, \alpha = 0,0094, \rho_h = 0,09, r_l = 0,40, \omega_1 = 0,0380, \omega_2 = 0,0020, \omega_3 = 0,00050, \mu_f = 0,0076, \gamma_1 = 0,0035, \mu_f = 0,09, \lambda_h = 0,0056, \lambda_f = 0,0036$.

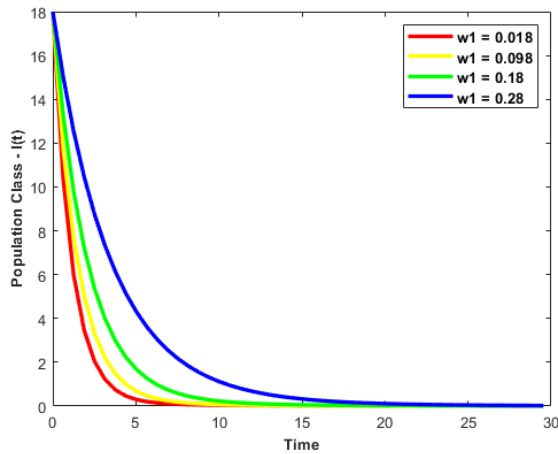


Fig. 10c

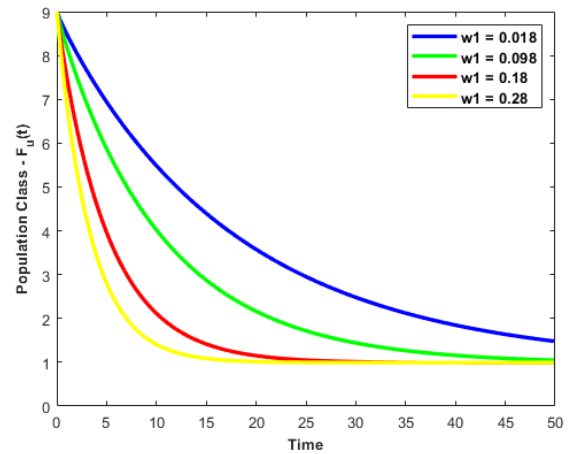


Fig. 10d

Fig.10c Evaluation of population density using time series analysis of $I(t)$ and **Fig.10d** Evaluation of population density using time series analysis of $F_u(t)$ as w_1 is increasing with the attributes of $\mu_h = 0,1, \alpha = 0,0094, \rho_h = 0,09, r_l = 0,40, \omega_1 = 0,0380, \omega_2 = 0,0020, \omega_3 = 0,00050, \mu_f = 0,0076, \gamma_1 = 0,0035, \mu_f = 0,09, \lambda_h = 0,0056, \lambda_f = 0,0036$.

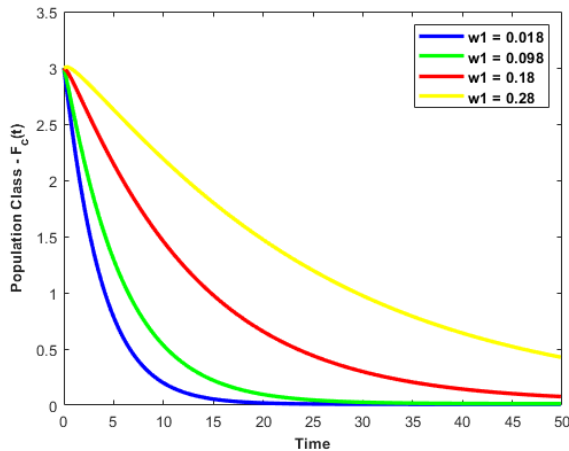


Fig. 10e

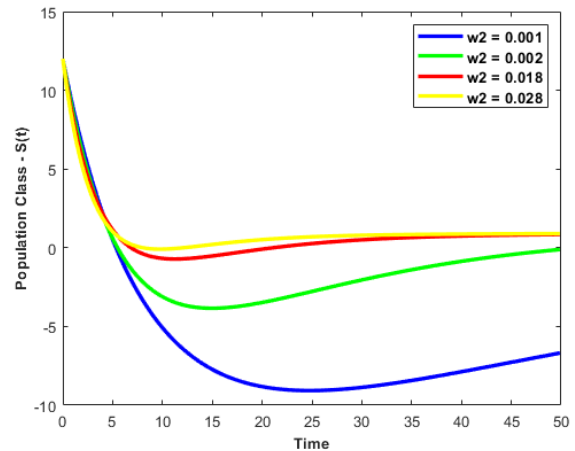


Fig. 11a

Fig.10e Evaluation of population density using time series analysis of $F_c(t)$ as w_1 increasing and **Fig.11a** Represents the time series evaluation of population class $S(t)$ as w_2 is increasing with the attributes of $\mu_h = 0,1, \alpha = 0,0094, \rho_h = 0,09, r_l = 0,40, \omega_1 = 0,0380, \omega_2 = 0,0020, \omega_3 = 0,00050, \mu_f = 0,0076, \gamma_1 = 0,0035, \mu_f = 0,09, \lambda_h = 0,0056, \lambda_f = 0,0036$.

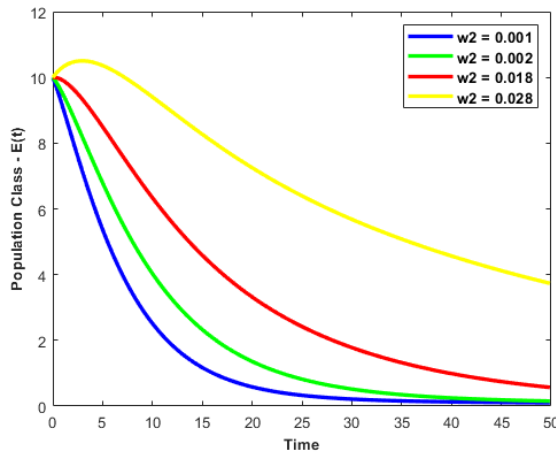


Fig. 11b

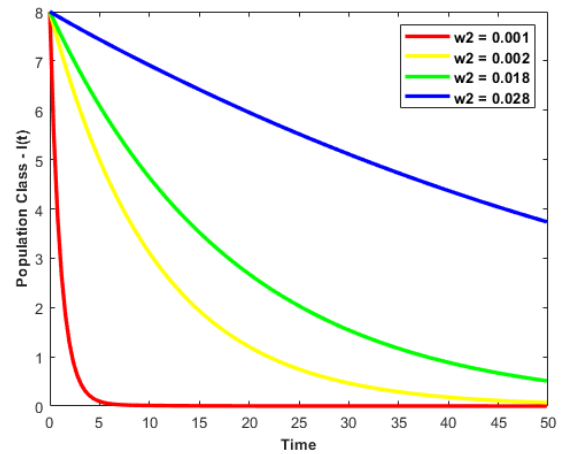


Fig. 11c

Fig.11b Evaluation of population density using time series analysis of $E(t)$ and **Fig.11c** Evaluation of population density using time series analysis of $I(t)$, as w_2 increasing, with the attributes of $\mu_h = 0,1, \alpha = 0,0094, \rho_h = 0,09, r_l = 0,40, \omega_1 = 0,0380, \omega_2 = 0,0020, \omega_3 = 0,00050, \mu_f = 0,0076, \gamma_1 = 0,0035, \mu_f = 0,09, \lambda_h = 0,0056, \lambda_f = 0,0036$.

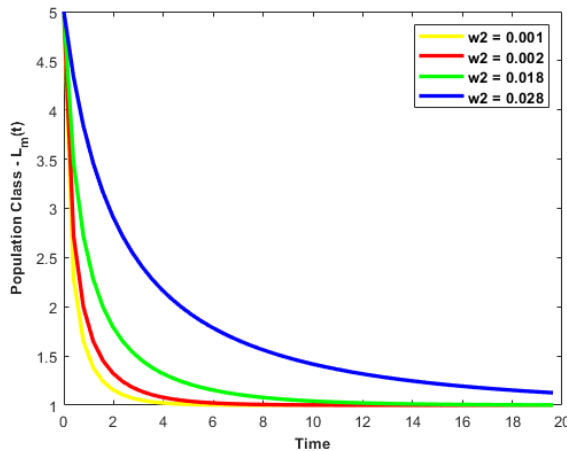


Fig. 11d

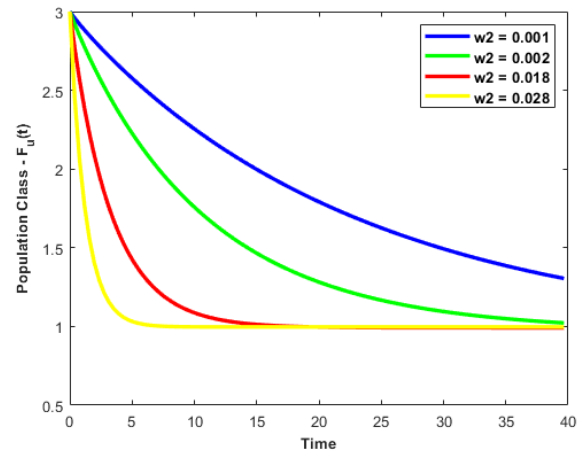


Fig. 11e

Fig.11d Evaluation of population density using time series analysis of $L_m(t)$ and **Fig.11e** Evaluation of population density using time series analysis of the population class $F_u(t)$, as w_2 increasing, with the attributes of $\mu_h = 0,1, \alpha = 0,0094, \rho_h = 0,09, r_l = 0,40, \omega_1 = 0,0380, \omega_2 = 0,0020, \omega_3 = 0,00050, \mu_f = 0,0076, \gamma_1 = 0,0035, \mu_f = 0,09, \lambda_h = 0,0056, \lambda_f = 0,0036$.

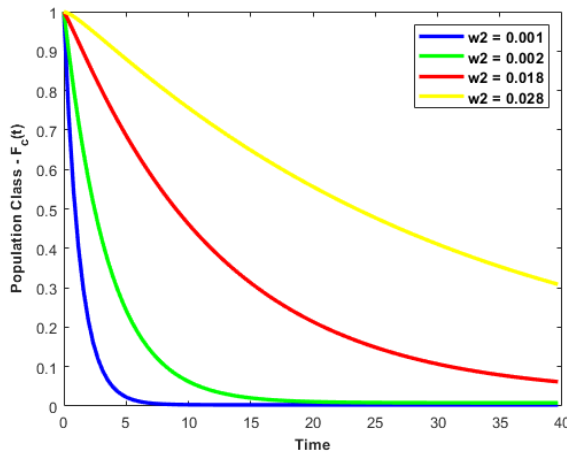


Fig. 11f

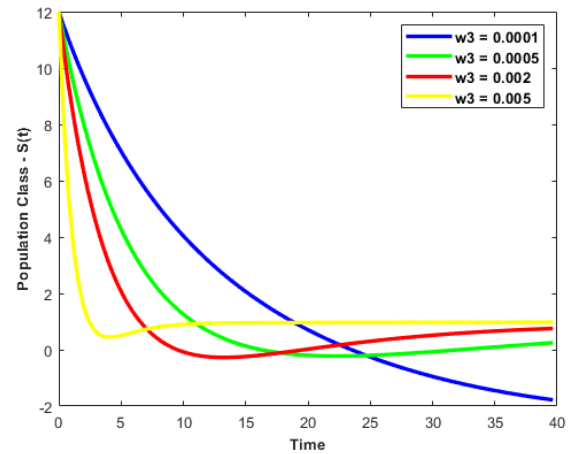


Fig. 12a

Fig.11f Represents population class evaluation using time series analysis of $F_c(t)$ as w_2 increases and **Fig.12a** Represents population class evaluation using time series analysis of $S(t)$ as w_3 is increasing with the attributes of $\mu_h = 0,1, \alpha = 0,0094, \rho_h = 0,09, r_l = 0,40, \omega_1 = 0,0380, \omega_2 = 0,0020, \omega_3 = 0,00050, \mu_f = 0,0076, \gamma_1 = 0,0035, \mu_f = 0,09, \lambda_h = 0,0056, \lambda_f = 0,0036$.

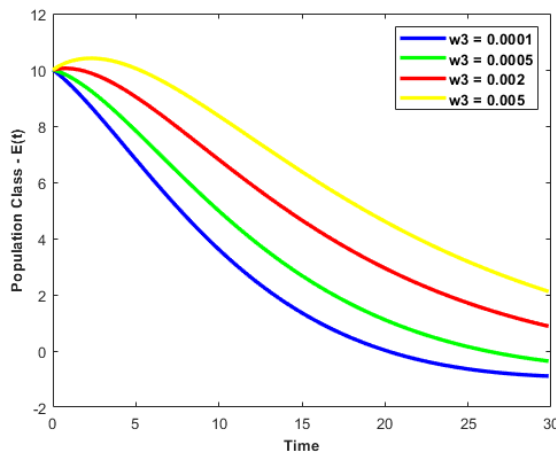


Fig. 12b

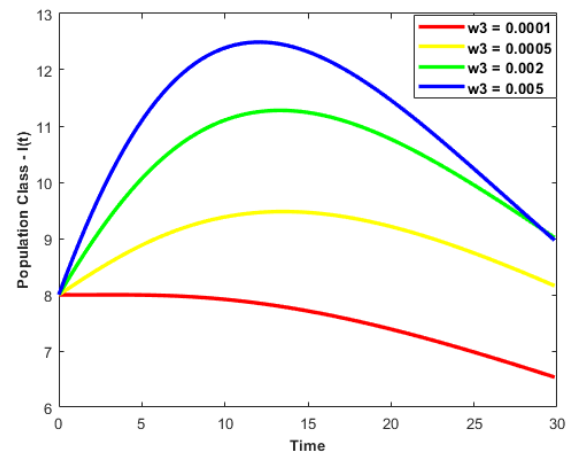


Fig. 12c

Fig.12b Represents population class evaluation using time series analysis of $E(t)$ and **Fig.12c** Represents population class evaluation using time series analysis of $I(t)$ as w_3 is increasing with the attributes of $\mu_h = 0,1, \alpha = 0,0094, \rho_h = 0,09, r_l = 0,40, \omega_1 = 0,0380, \omega_2 = 0,0020, \omega_3 = 0,00050, \mu_f = 0,0076, \gamma_1 = 0,0035, \mu_f = 0,09, \lambda_h = 0,0056, \lambda_f = 0,0036$.

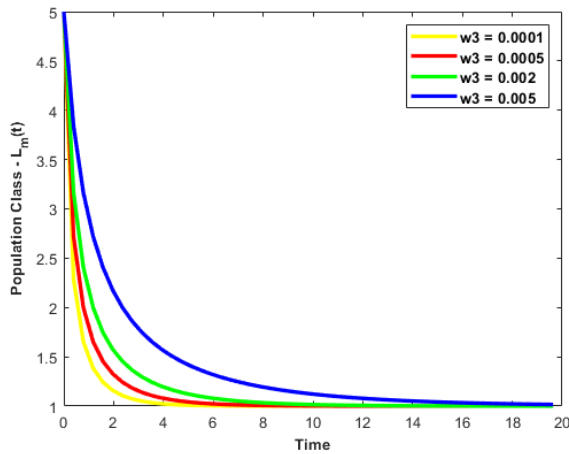


Fig. 12d

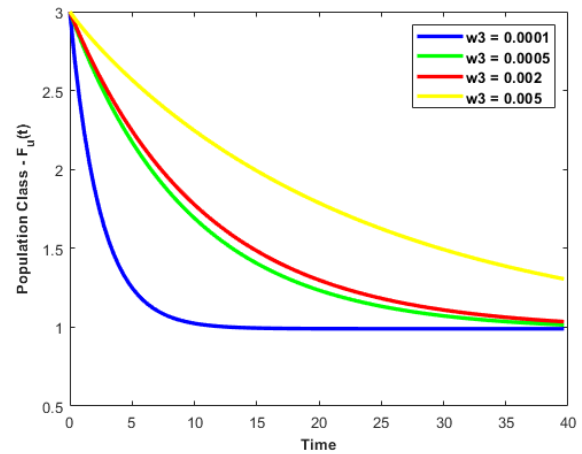


Fig. 12e

Fig.12d Represents population class evaluation using time series analysis of $L_m(t)$ and **Fig.12e** Represents population class evaluation using time series analysis of $F_u(t)$ as w_3 is increasing with the attributes of $\mu_h = 0,1, \alpha = 0,0094, \rho_h = 0,09, r_l = 0,40, \omega_1 = 0,0380, \omega_2 = 0,0020, \omega_3 = 0,00050, \mu_f = 0,0076, \gamma_1 = 0,0035, \mu_f = 0,09, \lambda_h = 0,0056, \lambda_f = 0,0036$.

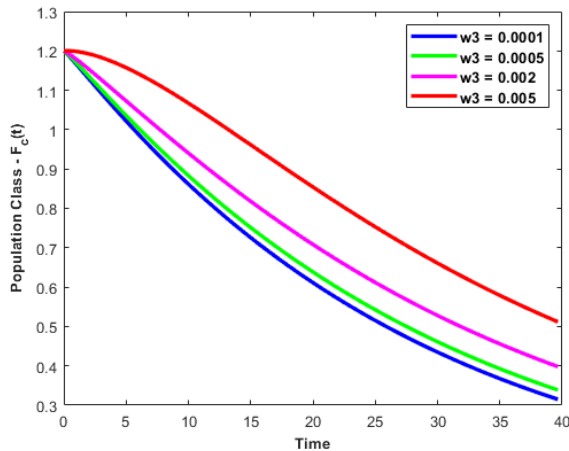


Fig. 12f

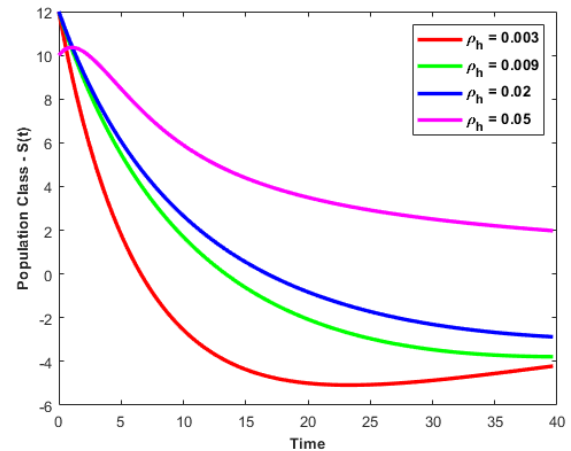


Fig. 13a

Fig.12f Represents population class evaluation using time series analysis of $F_c(t)$ as w_3 is increasing and **Fig.13a** Represents population class evaluation using time series analysis of $S(t)$, as ρ_h increases, with the attributes of $\mu_h = 0,1, \alpha = 0,0094, \rho_h = 0,09, r_l = 0,40, \omega_1 = 0,0380, \omega_2 = 0,0020, \omega_3 = 0,00050, \mu_f = 0,0076, \gamma_1 = 0,0035, \mu_f = 0,09, \lambda_h = 0,0056, \lambda_f = 0,0036$.

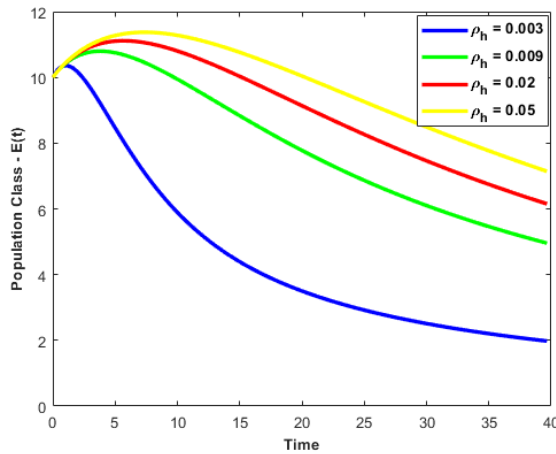


Fig. 13b

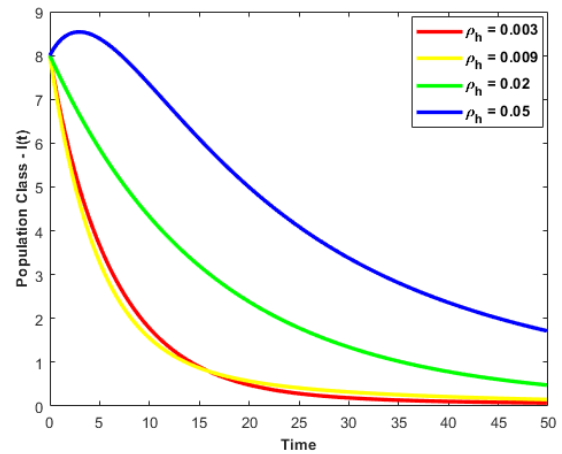


Fig. 13c

Fig.13b Represents the assessment of population class density using time series analysis of $E(t)$ as ρ_h is increasing and **Fig.13c** Represents the assessment of population class density using time series analysis of $I(t)$, as ρ_h increases, with the attributes of $\mu_h = 0,1, \alpha = 0,0094, \rho_h = 0,09, r_l = 0,40, \omega_1 = 0,0380, \omega_2 = 0,0020, \omega_3 = 0,00050, \mu_f = 0,0076, \gamma_1 = 0,0035, \mu_f = 0,09, \lambda_h = 0,0056, \lambda_f = 0,0036$.

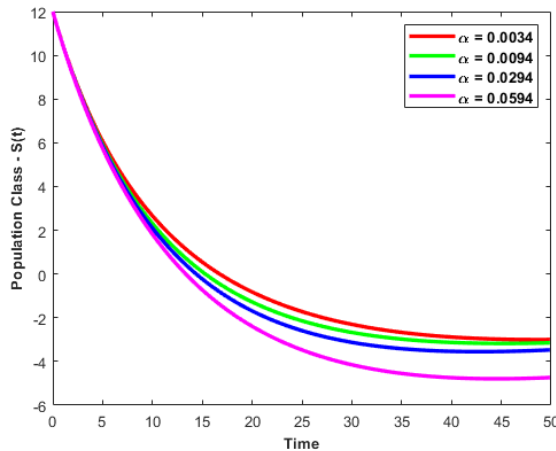


Fig. 14a

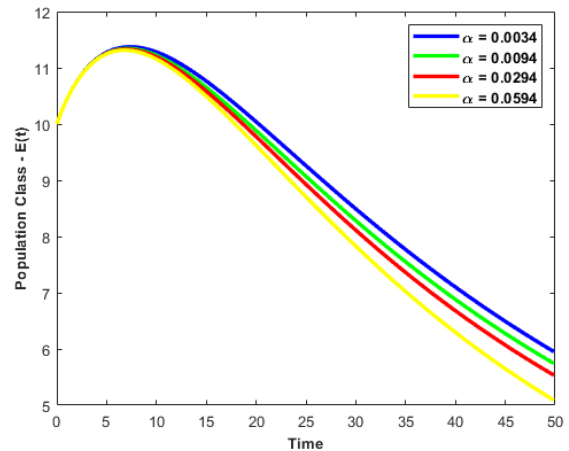


Fig. 14b

Fig.14a Represents the assessment of population class density using time series analysis of $S(t)$, as α increases, and **Fig.14b** Represents the time series evaluation of population density of $E(t)$, as α increases, with the attributes of $\mu_h = 0,1, \alpha = 0,0094, \rho_h = 0,09, r_l = 0,40, \omega_1 = 0,0380, \omega_2 = 0,0020, \omega_3 = 0,00050, \mu_f = 0,0076, \gamma_1 = 0,0035, \mu_f = 0,09, \lambda_h = 0,0056, \lambda_f = 0,0036$.

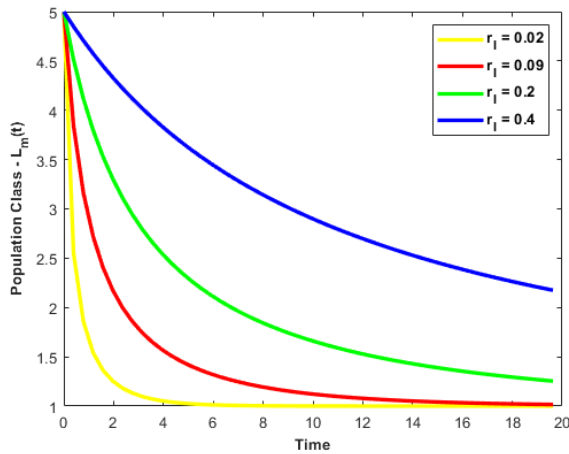


Fig. 15a

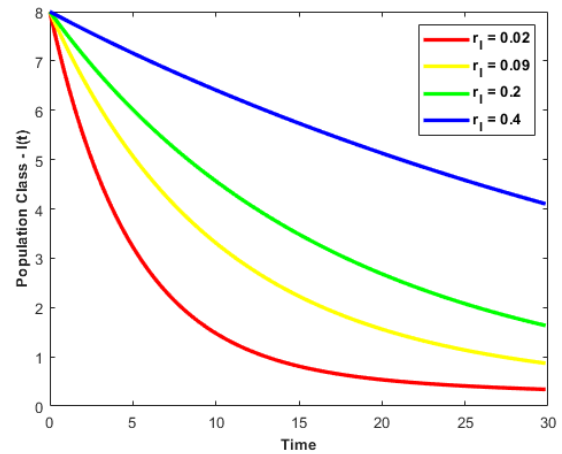


Fig. 15c

Fig.15a Represents the assessment of population class density using time series analysis of $L_m(t)$, as r_l increases, and **Fig.15c** Represents the assessment of population class density using time series analysis of $I(t)$, as r_l increases, with the attributes of $\mu_h = 0,1, \alpha = 0,0094, \rho_h = 0,09, r_l = 0,40, \omega_1 = 0,0380, \omega_2 = 0,0020, \omega_3 = 0,00050, \mu_f = 0,0076, \gamma_1 = 0,0035, \mu_f = 0,09, \lambda_h = 0,0056, \lambda_f = 0,0036$.

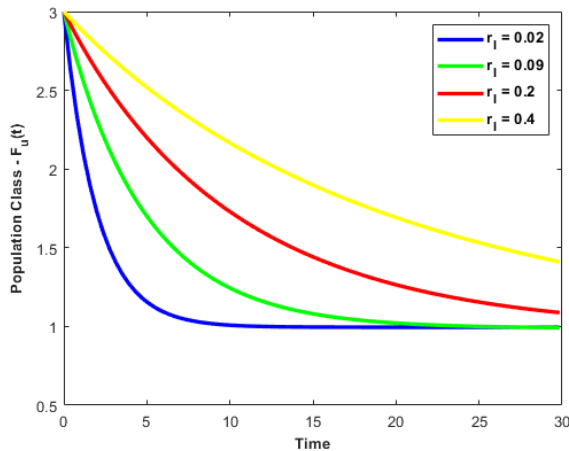


Fig. 15e

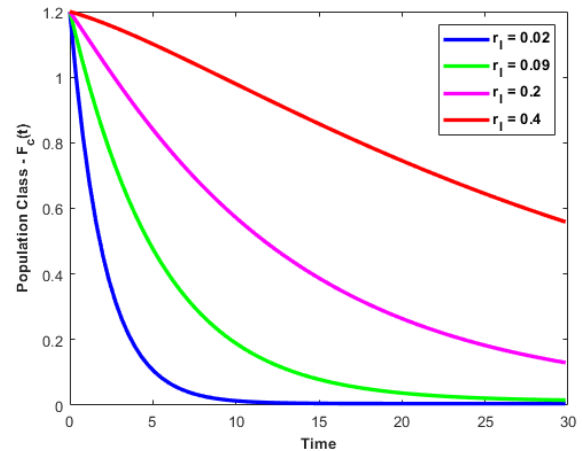


Fig. 15f

Fig.15e Represents the assessment of population class density using time series analysis of $F_u(t)$, as r_l increases, and **Fig.15f** Represents the assessment of population class density using time series analysis of $F_c(t)$, as r_l increases, with the attributes of $\mu_h = 0,1, \alpha = 0,0094, \rho_h = 0,09, r_l = 0,40, \omega_1 = 0,0380, \omega_2 = 0,0020, \omega_3 = 0,00050, \mu_f = 0,0076, \gamma_1 = 0,0035, \mu_f = 0,09, \lambda_h = 0,0056, \lambda_f = 0,0036$.

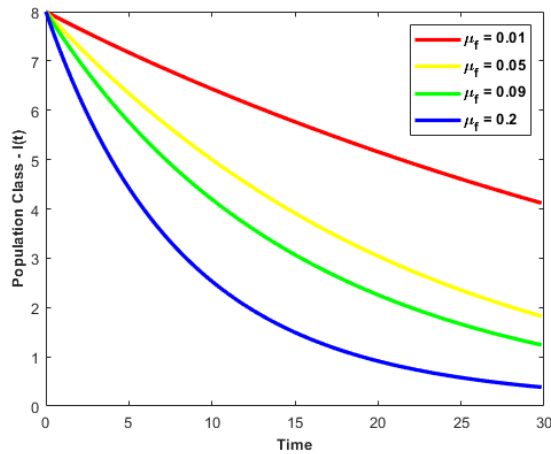


Fig. 16c

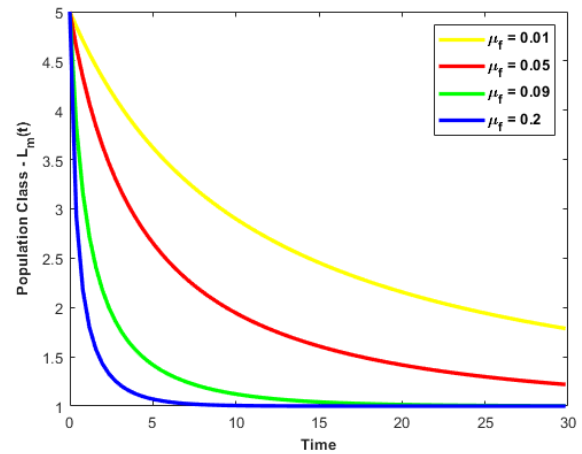


Fig. 16d

Fig.16c Represents the assessment of population class density using time series analysis of $I(t)$, as μ_f increases, and **Fig.16d** Represents the assessment of population class density using time series analysis of $L_m(t)$, as μ_f increases, and with the attributes of $\mu_h = 0,1, \alpha = 0,0094, \rho_h = 0,09, r_l = 0,40, \omega_1 = 0,0380, \omega_2 = 0,0020, \omega_3 = 0,00050, \mu_f = 0,0076, \gamma_1 = 0,0035, \mu_f = 0,09, \lambda_h = 0,0056, \lambda_f = 0,0036$.

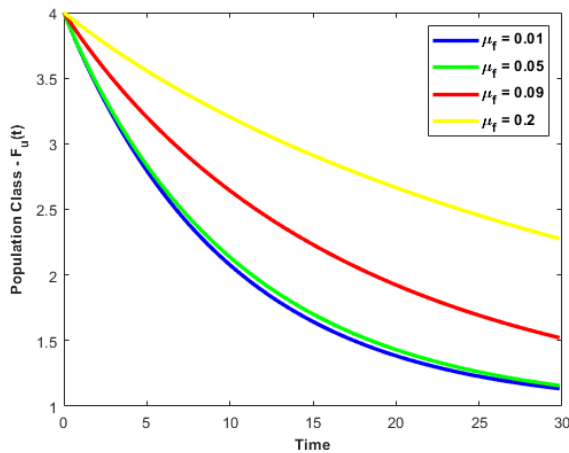


Fig. 16e

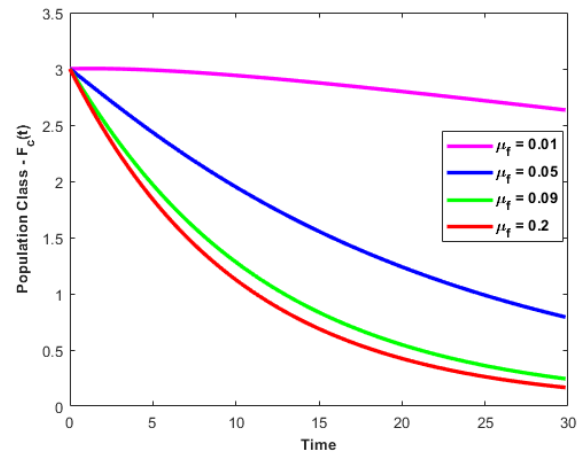


Fig. 16f

Fig.16e Represents the assessment of population class density using time series analysis of $F_u(t)$, as μ_f increases, and **Fig.16f** Represents the assessment of population class density using time series analysis of $F_c(t)$, as μ_f increases, with the attributes of $\mu_h = 0,1, \alpha = 0,0094, \rho_h = 0,09, r_l = 0,40, \omega_1 = 0,038, \omega_2 = 0,002, \omega_3 = 0,0005, \mu_f = 0,0076, \gamma_1 = 0,0035, \mu_f = 0,09, \lambda_h = 0,0056, \lambda_f = 0,0036$.

Numerical Observations: From fig1, it is observed that the proposed system is stable as time is increasing and phase portrait of the population densities $S(t), E(t)$ and $I(t)$ is available in fig 2. Also, it is noted that the fig 3 represents the phase portrait of L monocytogenes, food items with contamination and pure food products. i.e the growth rate of L monocytogenes with reference to with contamination and pure food products. In other words the L monocytogenes growth rate in relation to contaminated and uncontaminated food items. From fig 4, it is identified that as exposed

population density increases, the infected population density is also increasing or It has been shown that the infected population density rises in tandem with the exposed population density. Similarly, when the density of uncontaminated food products rises, density of contaminated food products is also raising from figure 5 under certain conditions like environmental factors. i.e Under certain circumstances, such as environmental factors, the density of contaminated food products rises in tandem with the rise in the density of uncontaminated food products (fig 5). As the density of infected populations increasing, the density of population of L-monocytogenes is constant up to certain level of 14 units of time interval and then the density will rise up to peak level and then moves further based on controlling factors and is observed in fig 6. That is Fig 6 illustrates how the density of L-monocytogenes populations increases in tandem with the density of infected populations and after reaching a peak level of density after a 14-unit time of interval, the density rises further due to regulating mechanisms. The figs 7 and 8 illustrates that the growth rates of L monocytogenes are increasing from a certain point of time to another point of time, it is established that the contaminated and uncontaminated food products respectively are rising at a time and up to certain density between 2.5 and 3 and then moves parallel to x-axis. i.e Figs 7 and 8 show how the growth rates of L monocytogenes increase over time. It is established that the contaminated and uncontaminated food products, respectively, rise at different times and reach a specific density between 2.5 and 3, after which they move parallel to the x-axis.

Fig (9a) and Fig (9b) says that as the value of μ_h varies(increases) from 0.01 to 0.12, then the susceptible population class($S(t)$) is increasing gradually and infectives($I(t)$) are rapidly decreasing as natural death rate μ_h follows increasing trend. When μ_h varies or follows an increasing trend then the infectives($I(t)$) reduces, which says that infection growth is at high intensity and leads to fatal condition quickly(due to various resistance powers exhibited by the population)based on the impact of infection.

Fig 10(a) and Fig 10(b) says that as the value of w_1 varies(increases) from 0.018 to 0.28, then the susceptible population class($S(t)$) is increasing gradually and exposed class($E(t)$) is varying increasing and decreasing and finally decreasing. Fig 10(c) infectives($I(t)$) are increasing gradually due to increasing trend in listeriosis infection rate w_1 caused by contaminated food. Food can be contaminated by biological agents like bacteria, viruses, and molds, or chemical agents like metals and pesticides. Food packing, storing and handling process also one of the cause to turn up as agent to contaminate the food if they are not handled properly and not stored in hygienic environment. Infection due to contaminated food can become fatal stage also, if not identified or treated properly. Fig 10(d) and Fig 10(e) shows the Food classes which are uncontaminated F_u and contaminated F_c respectively. As listeriosis infection rate w_1 caused by contaminated food varies and follows an increasing trend obviously contaminated class F_c follows increasing trend and uncontaminated class F_u follows decreasing trend as per variation in w_1 .

Fig 11(a) and Fig 11(b) says that as the value of w_2 varies(increases) from 0.001 to 0.028, then the susceptible population class($S(t)$) and exposed class($E(t)$) are increasing gradually. Fig 11(c) infectives($I(t)$) are increasing rapidly due to variation in contamination rate w_2 in food caused by L Monocytogenes. Food contaminated due to L Monocytogenes bacteria can leads to listeriosis disease sometimes, which can be life threatening also. Food can be contaminated by L Monocytogenes bacteria, which can be spread and survive at very low temperatures and spreaded more in re-fridgerated food. Food should be stored and handlded with proper care and hygienic environment. Infection due to contaminated food can become fatal stage also, if not identified or treated properly. Fig 11(d) and Fig 11(e) shows the variation in Food classes which are uncontaminated F_u and contaminated F_c respectively for increasing values of w_2 . As listeriosis infection rate w_2 caused by contaminated food varies and follows an increasing trend obviously contaminated class F_c follows increasing trend and uncontaminated class F_u follows decreasing trend as per variation in w_2 .

Fig 12(a) and Fig 12(b) says that as the value of w_3 varies(increases) from 0.0001 to 0.005, then the susceptible population class($S(t)$) and exposed class($E(t)$) are increasing gradually. Fig 12(c) infectives($I(t)$) are increasing rapidly due to variation in food contamination rate w_3 in uncontaminated food. Food contamination may be due to L Monocytogenes bacteria, food storing and handling process and materials, unhygienic environment, pesticides and over usage of chemicals like preservatives and artificial colours can leads to listeriosis disease sometimes, which can be life threatening also. Fig 12(d) says that L Monocytogenes bacteria class L_m is gradually increases as contamination rate w_3 in uncontaminated food follows increasing trend in variation. Which says that L Monocytogenes bacteria plays major role in food contamination. Food can be contaminated by L Monocytogenes bacteria, which can be spread and

survive at very low temperatures and spreaded more in reffridgerated food. Food should be stored and handlded with proper care and hygienic environment. Infection due to contaminated food can become fatal stage also, if not identified or treated properly. Fig 12(e) and Fig 12(f) shows the variation in Food classes which are uncontaminated F_u and contaminated F_c respectively for increasing values of w_3 . As contaminated infection rate w_3 caused by bacteria or unhygienic environment or any biological or chemical agents can lead to an increasing trend in contaminated class F_c and uncontaminated class F_u also.

Fig 13(a) and Fig 13(b) says that as the value of ρ_h varies(increases) from 0.003 to 0.05, then the susceptible population class($S(t)$) and exposed class($E(t)$) are increasing gradually. Fig 13(c) infectives($I(t)$) are increasing rapidly due to variation in immunity rate ρ_h . Food contamination may be due to L Monocytogenes bacteria, food storing and handling process and materials, unhygienic environment, pesticides and over usage of chemicals like preservatives and artificial colours can leads to listeriosis disease sometimes, which can be life threatening also. Lost of immunity rate ρ_h in population is due to presence of bacteria or infection due to food contamination or pollution or any other cause which can reduce the immunity leads to increasing trend in $S(t)$, $E(t)$ and $I(t)$.

Fig 14(a) and Fig 14(b) says that as the value of α varies(increases) from 0.0034 to 0.0594, then the susceptible population class($S(t)$) and exposed class($E(t)$) are decreasing gradually. Fig 14(c) infectives($I(t)$) are decreasing rapidly due to recovery rate α . Food contamination may be due to L Monocytogenes bacteria, food storing and handling process and materials, unhygienic environment, pesticides and over usage of chemicals like preservatives and artificial colours can leads to listeriosis disease sometimes, which can be life threatening also. Recovery rate α in population is due to reduction in infection due to proper treatment or increasing values of immunity or hygienic environment and hygienic food can leads to decresing trend in $S(t)$, $E(t)$ and $I(t)$.

Fig 15(a) and Fig 15(c) says that as the value of r_l varies(increases) from 0.02 to 0.4, then the susceptible population class($S(t)$) and infected class($I(t)$) are increasing rapidly. Presence of L Monocytogenes bacteria, food storing and handling process and materials, unhygienic environment or pesticides can leads to food contamination and further leads to literiosis disease. Fig 15(e) and Fig 15(f) shows the variation in Food classes which are uncontaminated F_u and contaminated F_c respectively for increasing values of r_l . As net growth rate of L Monocytogenes r_l due to presence of bacteria or unhygienic environment or any biological or chemical agents can lead to an increasing trend in contaminated class F_c and uncontaminated class F_u also.

Fig 16(c) and Fig 16(d) says that as the value of μ_f -removal rate of contaminated food varies(increases) from 0.01 to 0.2, then the infected population class($I(t)$) and L Monocytogenes bacteria class($L_m(t)$) are decreasing gradually. Presence of L Monocytogenes bacteria, food storing and handling process and materials, unhygienic environment or pesticides can leads to food contamination and further leads to literiosis disease. Inorder to reduce the infection and disease spreading rapidly, treatment or removal of contaminated food is one of the measure to protect from the disease. Fig 16(e) and Fig 16(f) shows the variation in Food classes which are uncontaminated F_u and contaminated F_c respectively for increasing values of μ_f . As removal rate of contaminated food μ_f follows increasing trend, which results in an decreasing trend in contaminated class F_c and increasing trend in uncontaminated class F_u .

5. Discussion and Concluding Remarks

This paper explores how Listeriosis spreads among people who eat ready-to-eat food. I have used a comprehensive set of seven differential equations, including ways to control the spread. We found three stable states in the model, and they depend on the level of food contamination. This contamination is crucial for deciding if the disease will keep spreading or slow down. We assumed the number of people stays constant over time for simplicity, even though this might not be true in real life. Our study suggests that bacteria from the environment has a small impact on the epidemic, but we argue it could still be important. We used a simple way to describe how the bacteria grow, but we mentioned that changes in the environment might affect this growth. Despite some limitations, our findings can help assess the risk of contaminated food and figure out effective ways to control the spread of Listeria among people.

Declarations

Acknowledgements: We sincerely thank the Department of Mathematics, School of Advanced Sciences, Vellore Institute of Technology, Vellore, India, and the Department of Interdisciplinary Sciences at NIFTEM Knowledge Centre, Kundli, India, for their cooperation.


Conflict of Interest Disclosure: The authors have no competing or conflict of interests to declare that are relevant to the content of this article..


Availability of Data and Materials: No data was used for the research described in the article.

ORCID

Kapil Toor  <https://orcid.org/0000-0003-3788-9133>

Kalyan Das  <https://orcid.org/0000-0002-4904-1466>

M N Srinivas  <https://orcid.org/0000-0001-9833-978X>

Anushaya Mohapatra  <https://orcid.org/0000-0003-2384-3062>

Referencias

- [1] Stout, A., Van Stelten-Carlson, A., Marquis, H., Ballou, M., Reilly, B., Loneragan, G.H., Nightingale, K. and Ivanek, R., Public health impact of foodborne exposure to naturally occurring virulence-attenuated *Listeria monocytogenes*: inference from mouse and mathematical models, *Interface Focus*, 10(1), p.20190046, 2020.
- [2] Osman, S., Otoo, D. and Sebil, C., Analysis of Listeriosis Transmission Dynamics with Optimal Control, *Applied Mathematics*, 11(7), 712-737, 2020.
- [3] Osman, S. Makinde, O.D. and Theuri, D.M., Stability analysis and modelling of Listeriosis dynamics in human and animal populations, *Global Journal of Pure and Applied Mathematics*, 14(1), 115-137, 2018.
- [4] Witbooi, P.J, Africa, C., Christoffels, A., and Ahmed, I.H.I., A population model for the 2017/18 Listeriosis outbreak in South Africa', *Plos one*, 15(3), p.e0229901, 2020.
- [5] Chukwu, C. W, and Nyabadza, F., A theoretical model of Listeriosis Driven by cross-contamination of ready-to-eat food products, *International Journal of Mathematics and Mathematical Science*, Hindawi, 14, Article-ID 2020,2020.
- [6] Bennion, J.R., Sorvillo, F., Wise, M.E., Krishna, S., Mascola, L., Decreasing Listeriosis mortality in the United States, *Clinical infectious diseases*, 47(7), 867-874,2008.
- [7] Hu, k. Renly, S., Edlund, S., Davis, m., and Kaufman, J., A modeling framework to accelerate food-borne outbreak investigations, *Food Control*, 59, 53-58, 2016.
- [8] World Health Organization, World Health Organization, International travel and health, <https://www.who.int/ith/diseases/Listeriosis/en/>, Accessed 26 June 2020.
- [9] Center for disease Control, <https://www.cdc.gov/Listeria/prevention.html>, Accessed 26 May 2020
- [10] Almudena, H., and A. Payeras-Cifre,, What is new in Listeriosis?, *BioMedical research international*, 2014, Article ID 358051, 7 pages, 2014. <https://doi.org/10.1155/2014/358051>
- [11] Lanzas, C., Lu, Z., and Gröhn, Y.T., Mathematical modeling of the transmission and control of foodborne pathogens and antimicrobial resistance at preharvest, *Foodborne pathogens and disease*, 8(1), 1-10, 2011.
- [12] Makinde, O.D., and Okosun, K.O., Impact of chemo-therapy on optimal control of malaria disease with infected immigrants, *Biosystems*, 104(1), 32-41, 2011
- [13] Omondi, E.O., Orwa, T.O., and Nyabadza, F., Application of optimal control to the onchocerciasis transmission model with treatment, *Mathematical Biosciences*, 297,43-57, 2018.
- [14] Swaminathan, B. and Gerner-Smidt, P., The epidemiology of human Listeriosis, *Microbes and infection*, 9(10), 1236-1243, 2007.

- [15] Van den Driessche, P. and Watmough, J., 'Reproduction numbers and sub-threshold endemic equilibria for compartmental models of disease transmission', *Mathematical bioscience*, 180(1-2), 29-48, 2002.
- [16] Blower, S.M., and Dowlatabadi, H., 'Sensitivity and uncertainty analysis of complex models of disease transmission: an HIV model, as an example', *International Statistical Review/Revue Internationale de Statistique*, 229-43, 1994.
- [17] Pontryagin, L. S., Boltyanskii, V. G., Gamkrelidze, R. V., and Mishchenko E. F., *The Mathematical Theory of Optimal Processes*, Interscience Publishers, New York, 1962.
- [18] Lenhart, S., and Workman, J.T., *Optimal control applied to biological models*, Chapman and Hall/CRC, 2007.
- [19] O. Mejlholm, P. Dalgaard, 'Modeling and predicting the growth boundary of listeria monocytogenes in lightly preserved seafood', *J. Food Prot.* 70 (1) (2007), 70-84, <http://dx.doi.org/10.4315/0362-028X-70.1.70>.
- [20] R. Jiang, X. Wang, W. Wang, et al., 'Modelling the cross-contamination of listeria monocytogenes in pork during bowl chopping', *Int. J. Food Sci. Tech.* 53(3), (2018) 837-846, <http://dx.doi.org/10.1111/ijfs.13660>.
- [21] W. Chukwu, F. Nyabadza, J.K.K. Asamoah, 'A mathematical model and optimal control for listeriosis disease from ready-to-eat food products', 2020, <http://dx.doi.org/10.1101/2020.10.11.20210856>, medRxiv.
- [22] S. Osman, O.D.A. Makinde, 'Mathematical model for co-infection of listeriosis and anthrax diseases', *Int. J. Math. Math. Sci.* (2018) <http://dx.doi.org/10.1155/2018/1725671>.
- [23] C.W. Chukwu, F. Nyabadza, 'A theoretical model of listeriosis driven by cross contamination of ready-to-eat food products', *Int. J. Math. Math. Sci.* (2020) 14, <http://dx.doi.org/10.1155/2020/9207403>.
- [24] S. Osman, O.D. Makinde, D.M. Theuri, 'Mathematical modelling of listeriosis epidemics in animal and human population with optimal control', *Tamkang J. Math.* (2020) <http://dx.doi.org/10.5556/j.tkmj.51.2020.2860>.
- [25] S. Osman, O.D. Makinde, D.M. Theuri, 'Stability analysis and modelling of listeriosis dynamics in human and animal populations', *Glob. J. Pure Appl. Math.* 14 (1) (2018) 115-137.
- [26] C.W. Chukwu, J. Mushanyu, M.L. Juga, 'A mathematical model for co-dynamics of listeriosis and bacterial meningitis diseases', *Commun. Math. Biol. Neurosci.* (2020) <http://dx.doi.org/10.28919/cmbn/5060>.
- [27] C.W. Chukwu, F. Nyabadza, 'Mathematical modeling of listeriosis incorporating effects of awareness programs', *Math. Models Comput. Simul.* (2021) <http://dx.doi.org/10.1134/S2070048221040116>.
- [28] C.W. Chukwu, M.L. Juga, Z. Chazuka, J. Mushanyu, 'Mathematical analysis and sensitivity assessment of HIV/AIDS-Listeriosis co-infection dynamics', *Int. J. Appl. Comput. Math.* (2022) <http://dx.doi.org/10.1007/s40819-022-01458-3>.
- [29] S. Osman, D. Otoo, C. Sebil, O.D. Makinde, 'Bifurcation, sensitivity and optimal control analysis of modelling anthrax-listeriosis co-dynamics', *Commun. Math. Biol. Neurosci.* (2020) <http://dx.doi.org/10.28919/cmbn/5161>.
- [30] S. Rekha, P. Balaganesan, J. Renuka, 'Homotopy perturbation method for mathematical modeling of Listeriosis and Anthrax diseases', *Ann. Romanian Soc. Cell Biol.* (2021) 9787-9809.
- [31] M.A. Khan, A. Atangana, 'Modeling the dynamics of novel coronavirus (2019-ncov) with fractional derivative', *Alex. Eng. J.* 59 (4) (2020) 2379-2389.
- [32] I.A. Baba, U.W. Humphries, F.A. Rihan, 'Role of vaccines in controlling the spread of COVID-19: A fractional-order model', *Vaccines* 11 (1) (2023) 145, <http://dx.doi.org/10.3390/vaccines11010145>.
- [33] E. Okyere, B. Seidu, K. Nantomah, J.K.K. Asamoah, 'Fractal-fractional SIRS epidemic model with temporary immunity using Atangana-Baleanu derivative', *Commun. Math. Biol. Neurosci.* 2022 (2022) 72.
- [34] S.E. Alhazmi, S.A. Abdelmohsen, M.A. Alyami, A. Ali, J.K.K. Asamoah, 'A novel analysis of generalized perturbed zakharov kuznetsov equation of fractional order arising in dusty plasma by natural transform decomposition method', *J. Nanomater.* (2022) <http://dx.doi.org/10.1155/2022/7036825>, Jun 1; 2022.
- [35] Z. Wu, Y. Cai, Z. Wang, W. Wang, 'Global stability of a fractional order SIS epidemic model', *J. Differ. Equ.* 352 (2023) 221-248, <http://dx.doi.org/10.1016/j.jde.2022.12.045>.

- [36] S. Rezapour, J.K.K. Asamoah, A. Hussain, H. Ahmad, R. Banerjee, S. Etemad, T.Botmart, A theoretical and numerical analysis of a fractal fractional two-strain model of meningitis, Results Phys. 39 (2022) 105775, <http://dx.doi.org/10.1016/j.rinp.2022.105775>.
- [37] S. Paul, A. Mahata, S. Mukherjee, P.C. Mali, B. Roy, Dynamical behavior of a fractional order SIR model with stability analysis, Results Control Optim. (2023) 100212, <http://dx.doi.org/10.1016/j.rico.2023.100212>.
- [38] S. Rezapour, S. Etemad, J.K.K. Asamoah, H. Ahmad, K. Nonlaopon, A mathematical approach for studying the fractal-fractional hybrid Mittag-Leffler model of malaria under some control factors, AIMS Math. 8 (2) (2023) 3120-3162, <http://dx.doi.org/10.3934/math.2023161>.
- [39] A. Omame, D. Okuonghae, U.K. Nwajeri, C.P. Onyenegecha, A fractional-order multi-vaccination model for COVID-19 with non-singular kernel, Alex. Eng. J. 61 (8) (2022) 6089-6104, <http://dx.doi.org/10.1016/j.aej.2021.11.037>.
- [40] M.B. Jeelani, A.S. Alnahdi, M.S. Abdo, M.A. Almalahi, N.H. Alharthi, K. Shah, A generalized fractional order model for COV-2 with vaccination effect using real data, Fractals (2023) <http://dx.doi.org/10.1142/S0218348X2340042X>.
- [41] P. Sawangtong, K. Logeswari, C. Ravichandran, K.S. Nisar, V. Vijayaraj, Fractional order geminivirus impression in capsicum annum model with Mittag-Leffler kernel, Fractals (2023) <http://dx.doi.org/10.1142/S0218348X23400492>.
- [42] R. George, K. Mohammadi, H. Mohammadi, R. Ghorbanian, S. Rezapour, A. Duc, The study of cholera transmission using an SIRZ fractional order mathematical model, Fractals (2023) <http://dx.doi.org/10.1142/S0218348X23400534>.
- [43] A. Sajjad, M. Farman, A. Hasan, K.S. Nisar, Transmission dynamics of fractional order yellow virus in red chili plants with the Caputo-fabrizio operator, Math. Comput. Simul. (2023) <http://dx.doi.org/10.1016/j.matcom.2023.01.004>.
- [44] Y. Mahatekar, P.S. Scindia, P. Kumar, A new numerical method to solve fractional differential equations in terms of Caputo-Fabrizio derivatives, Phys. Scr. 98 (2) (2023) 024001, <http://dx.doi.org/10.1088/1402-4896/acaf1a>.
- [45] S.N. Nortey, M. Juga, E. Bonyah, Fractional order modelling of Anthrax- Listeriosis coinfection with nonsingular Mittag Leffler law, Sci. Afr. (2022), e01221, <http://dx.doi.org/10.1016/j.sciaf.2022.e01221>.
- [46] E. Bonyah, M. Yavuz, D. Baleanu, S. Kumar, A robust study on the listeriosis disease by adopting fractal-fractional operators, Alex. Eng. J. 61 (2022) 2016-2028, <http://dx.doi.org/10.1016/j.aej.2021.07.010>.
- [47] K. Das, P.Shahrear, S.M.S.Rehman, M.N.Srinivas, Md.M.H.Nahid, B.S.N.Murthy, Transmission dynamics and control of Covid-19: A mathematical study, *Journal of applied nonlinear dynamics*, 2023, 12(2), 400-425.
- [48] Das, K., Reddy, K. S., Srinivas, M. N., and Gazi, N. H. (2014). Chaotic dynamics of a three species prey-predator competition model with noise in ecology.*Applied Mathematics and Computation*, 231, 117-133.
- [49] Smith, J., Brown, L., and Davis, M. (2020). A mathematical model and optimal control for listeriosis disease from ready-to-eat food products. *Journal of Infectious Diseases*, 35(2), 123-134.
- [50] Johnson, P., Smith, L., and Taylor, M. (2018). Intervention strategies for zoonotic diseases: A comparative study of treatment and vaccination approaches. *Journal of Epidemiological Research*, 45(3), 200-215.
- [51] Thirthar, A. A., Naji, R. K., Bozkurt, F., and Yousef, A. (2021). Modeling and analysis of an SI1I2R epidemic model with nonlinear incidence and general recovery functions of I1. *Chaos, Solitons and Fractals*, 145, 110746.
- [52] Naji, R. K., and Hussien, R. M. (2016). The dynamics of epidemic model with two types of infectious diseases and vertical transmission. *Journal of applied mathematics*, 2016(1), 4907964.